

Fig. 1 (continued).

3.4. PDE4-specific activity

We investigated the activity of the PDE4 mutants found in patients to determine whether the mutations affect the cAMP-hydrolyzing capability of the enzyme. Five distinct PDE4D mutant constructs (Q164P, L166S, T523A, G609D, and I614T; based on PDE4D5 [47], Table 3) were overexpressed in HEK293 cells and

lysates containing equal amounts of WT and mutant PDE4D proteins were used to assess the proteins' ability to hydrolyze cAMP (Fig. 3A). Relative to WT PDE4D, all the PDE4D mutants exhibited markedly diminished cAMP-hydrolyzing activity. Therefore, inserting the PDE4 gene mutations found in patients with acrodysostosis without hormone resistance into PDE4D4 severely compromised the catalytic activity of PDE4D4.

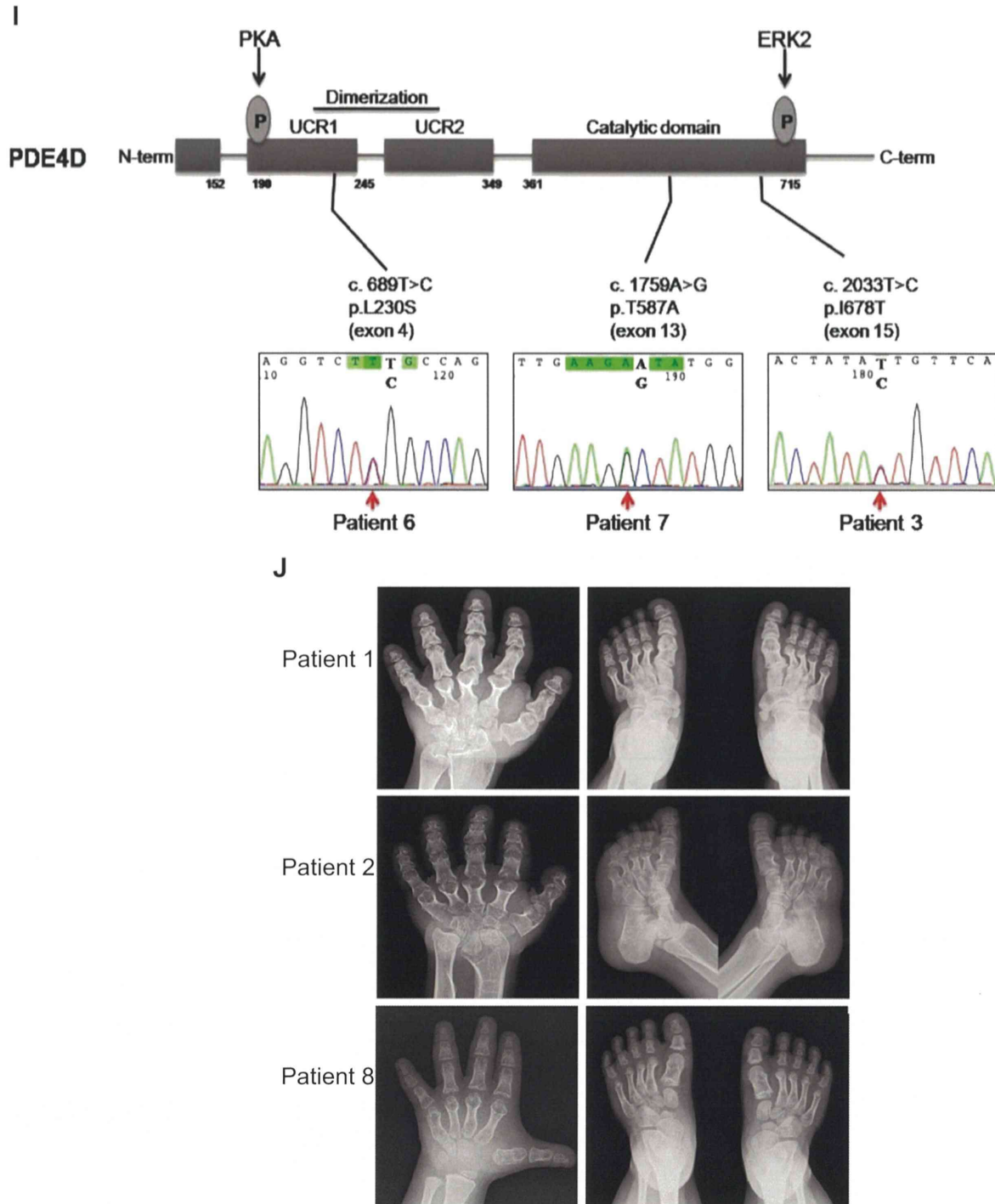


Fig. 1 (continued).

Next, we measured the cAMP PDE activity in EBV-immortalized lymphocytes from control subjects and patients. We determined the total cAMP-hydrolyzing activity in the presence or absence of the pan-PDE inhibitor IBMX, which inhibits all cAMP-hydrolyzing PDEs except PDE8 [8]. We also conducted these assays in the presence of the PDE4-specific inhibitor Rolipram, which enabled us to estimate the fraction of total PDE activity that was due to PDE4 [55]. This allowed us to compare both total PDE and PDE4-specific cAMP-hydrolyzing activity in the control subject and in the PDE4D-mutated patient 6 (Fig. 4). Surprisingly, we found that patient 6 exhibited total PDE and PDE4-specific activities that were similar to those of the control subject. This may be

Table 2

The average binding affinities of PDE4D WT and mutants (p.Gly673Asp and p.Ile678Thr). Standard deviations of the binding affinity shown in parenthesis were calculated based on 30 flexible docking simulations. The WT protein is slightly more stable with cAMP (by approximately 0.17 kcal/mol) than the 2 mutants. The number of successful bindings of cAMP to the binding pocket is 30 for WT protein and 4 and 9 for the 2 mutants.

Models	Average binding affinity (kcal/mol)	Number of successful binding of the 30 trials
WT	−8.70 (±0.000)	30
p.Gly673Asp (Pt 2)	−8.51 (±0.311)	4
p.Ile678Thr (Pt 1)	−8.56 (±0.292)	9

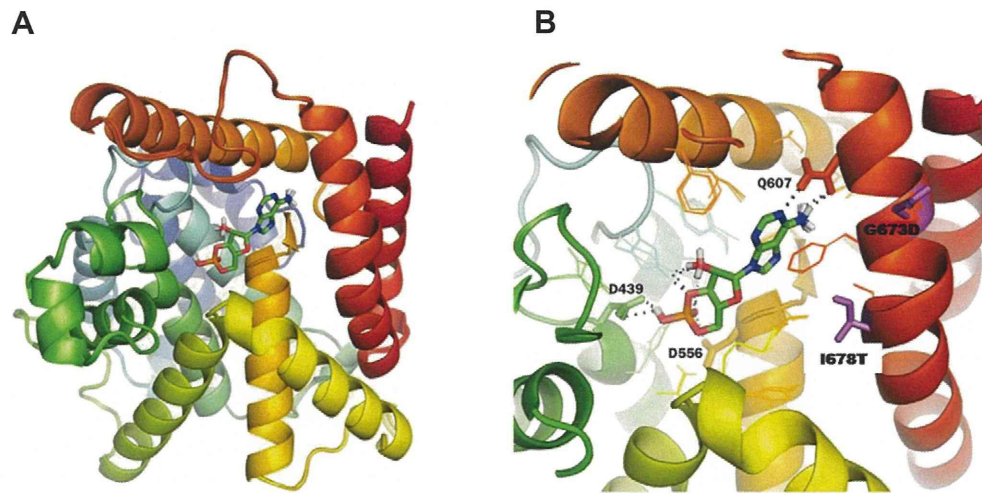


Fig. 2. Three dimensional structural models of the catalytic domain of PDE4D. Panel A shows the protein model of WT PDE4D with cAMP and panel B shows the models of the mutants (p.Gly673Asp and p.Ile678Thr) with cAMP. The 3 structures were superposed using the pyMOL program, and the cAMP ligand is positioned at the lowest-energy binding site found in the docking simulation. The binding between the protein and cAMP is shown in detail. D503, D620, and Q671 are known to be conserved binding residues. Side-chains of G673D and I678T are depicted by purple stick figures on the right-hand side of the binding pocket.

because PDE4D isoforms contribute little to the total PDE4 activity in these cells, or because in patient 6 the loss of PDE4D activity was compensated for by the up-regulation of catalytically functional PDE4 from other subfamilies.

3.5. Expression of PDE4 and its isoforms in patient cells

We sought to determine if the expression of PDE4 from other subfamilies was altered in patient 6, and we found a dramatic increase in PDE4C expression in the patient (Fig. 4D). By contrast, no changes were detected in the expression of PDE4A and PDE4B subfamilies (Fig. 4D). We also noted that *PDE4D5* and *PDE4D11* mRNA levels in

the cells from patient 6 were double than that in control cells (Fig. 4D). This increase in transcripts correlated with an elevated PDE4D5 protein level relative to control, which was shown by staining by a PDE4D5-specific antibody (Fig. 4E).

Our expression-analysis data indicate that in patient 6, the loss of PDE4D activity was compensated for not only through the up-regulation of PDE4D5 and PDE4D11, which would be catalytically compromised, but also through the up-regulation of PDE4C. We propose that these changes help compensate for the reduced catalytic activity of PDE4D isoforms and could explain why total PDE4 activity was almost identical in the EBV-immortalized lymphocytes obtained from the control subject and patient 6 (Fig. 4, A–C).

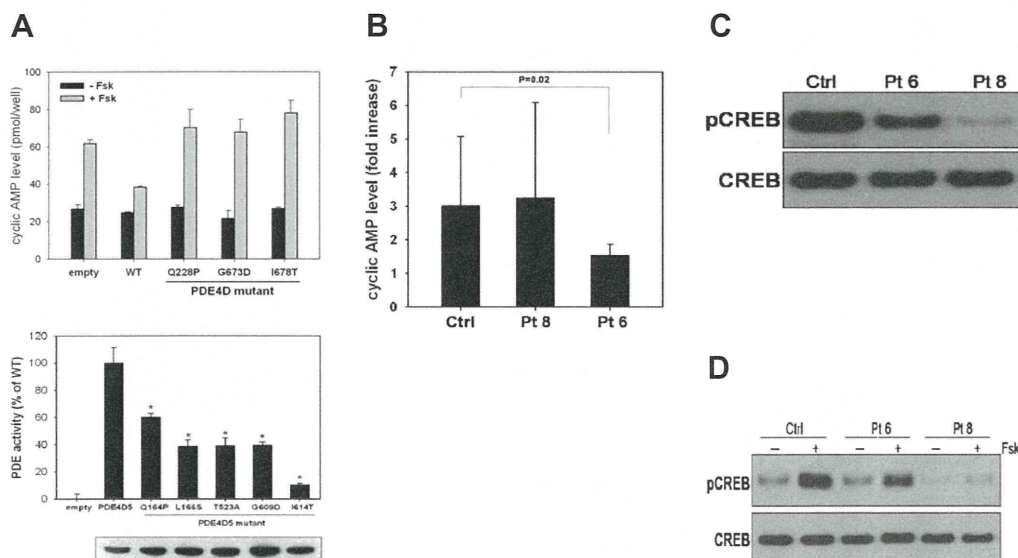


Fig. 3. Phosphorylation of cAMP responsive element-binding (CREB) protein in acrodysostosis patients. A. Functional studies on PDE4D in HEK 293 cells. Panel A shows measurement of cAMP in HEK293 cells transfected PDE4D5 WT and mutant constructs. Because the PDE4D isoform is the major species that has cAMP-hydrolyzing activity, we analyzed whether overexpressing recombinant WT or mutant PDE4D affects the cellular level of cAMP in HEK293 cells after treatment with the adenylyl-cyclase activator forskolin (Fsk, 10 μ M). WT PDE4D decreased cellular cAMP levels, but overexpressed Q228P-, G673D-, and I678T-PDE4D mutants did not. Panel B shows the total PDE activity of PDE4D constructs. Compared to WT, all of PDE4D mutants had significantly reduced PDE activity. The results are shown as means \pm SD. B. Levels of cAMP in EBV-transformed lymphocytes of control subject, patient 8, and patient 6 after treatment with forskolin (Fsk, 10 μ M). In cells from patient 6 (with L230S mutation), cAMP levels showed a statistically significant decrease compared to control EBV-transformed lymphocytes. C. Phosphorylated CREB levels in control, patient 6, and patient 8 cells; both patients had lower than control pCREB levels. D. Diminished pCREB levels in patient cells were observed clearly after stimulating with Fsk for 30 min.

Table 3
PDE4D isoforms with mutation residue numbers.

PDE4D4	D1	D2	D3	D5	D6	D7	D8	D9	D10*	D11*
Type	Short	Short	Long	Long	Short	Long	Long	Long	Short	Short
Q228P	N/A	N/A	92	164	N/A	167	106	98	N/A	118
L230S	N/A	N/A	94	166	N/A	169	108	100	N/A	120
T587A	363	285	451	523	296	526	465	457	283	477
G673D	449	371	537	609	382	612	551	543	369	563
I678T	454	376	542	614	387	617	556	548	374	568

N/A – not applicable as mutation not in N-terminal portion of short form sequence. All clones are human except where indicated*, which are murine clones. The GenBank flat file numbers used are indicated in parentheses PDE4D1 (NP_001184151), PDE4D2, PDE4D3 (NP_006194), PDE4D4 (NP_001098101), PDE4D5 (NP_001184147), PDE4D6 (NP_001184152), PDE4D7 (NP_001159371), PDE4D8 (NP_001184148), PDE4D9 (NP_001184149), PDE4D10 (ABG57277) and PDE4D11 (ACA66114).

3.6. Immunofluorescent staining of EBV-transformed B cells

Immunofluorescence staining for PDE4D and the PDE4D scaffold proteins [7,22,56], RACK1 and β -arrestin, demonstrated similar colocalization in patient and control cells of PDE4D (Fig. 5).

3.7. PDE4D-KO rats

The role of PDE4D mutations in acrodysostosis was clarified by generating a PDE4D-KO rat. Body lengths measured at the ages of 3 and 5 weeks indicated significantly stunted growth in both male and female KO rats relative to WT rats (3 weeks: male to male, $P < 0.001$, female to female, $P < 0.001$; 5 weeks: male to male, $P < 0.001$, female to female, $P = 0.002$, Fig. 6A); stunted growth was

observed in the KO and heterozygous rats compared to WT rats at 3 weeks ($P < 0.001$, Fig. 6B).

Skeletal radiographs of 10-week-old KO rats showed that the distal parts of the forelimbs (radius and palm) were shorter than in WT rats, and that all metacarpals and phalanges were shorter in KO rats than in WT rats (Fig. 6C and D).

4. Discussion

In this study, we have shown that PDE4D mutations are associated with acrodysostosis without apparent hormone resistance. The PDE4D gene encodes proteins that critically regulate $G\alpha$ -cAMP signaling by modulating the compartmentalization of this key signaling system through targeted cAMP degradation [7,19,57].

PDE4D-family enzymes hydrolyze cAMP and tightly regulate the $G\alpha$ -cAMP signal transduction pathway that employs PKA and Epac as its core effectors [7,54]. The PDE4D gene is associated with several distinct diseases or traits including ischemic stroke, neuroticism, asthma, and esophageal cancer [58–61]. Our work and 2 recently reported studies [62,63] implicate PDE4D as a third gene associated with $G\alpha$ -cAMP signaling-linked disorders; the others are GNAS, whose mutations are implicated in PHP-1a, pseudo-pseudohypoparathyroidism (PPHP), and progressive osseous heteroplasia (POH), and whose methylation defect is implicated in PHP-1b, and PRKARIA, a nonsense mutation which is associated with acrodysostosis with hormone resistance [5,64].

From the clinical standpoint, our study and the 2 recent studies indicate that skeletal dysplasia may be causally related to hormonal resistance through a signal transduction pathway. At one end of hormonal resistance lies PHP-1b, which is manifested as a resistance to hormones like PTH and TSH. However, the skeletal manifestations associated with

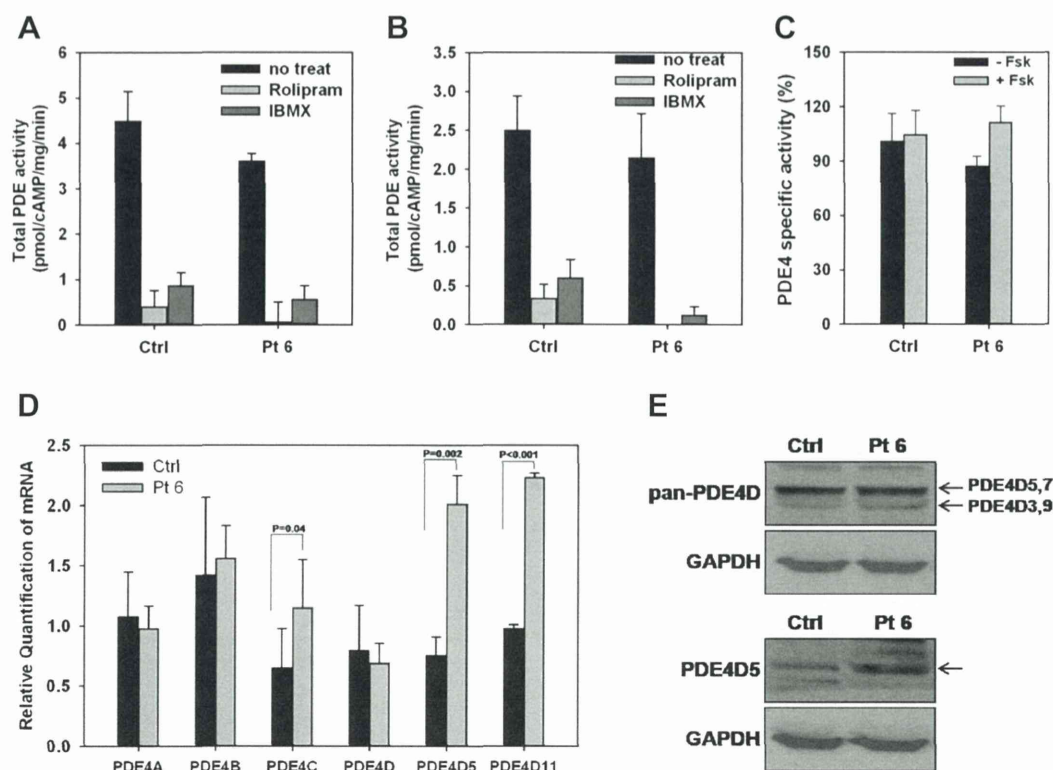


Fig. 4. Normal PDE4-specific activity in the acrodysostosis patient. EBV-transformed lymphocytes of control subject and patient 6 were harvested to measure the total PDE activity before (A) and after (B) Fsk stimulation (10 μ M, 30 min) and also PDE4-specific activity (C). We measured the total cAMP-hydrolyzing activity in the presence or absence of the pan-PDE inhibitor IBMX (100 μ M), and in the presence of the PDE4-specific inhibitor rolipram (10 μ M) to estimate the PDE4 fraction of the total PDE activity. In patient and control cells, total PDE and PDE4-specific activities were not different (means \pm SD shown) (D). Because PDE4 activity levels were the same in the control subject and patient 6, we determined the expression of PDE4 and PDE4D isoform mRNAs in the patient. PDE4C isoform was increased in patient 6 in a statistically significant manner, and the expression of PDE4D isoforms was also increased; * $P < 0.05$, ** $P < 0.005$ (E). PDE4D and PDE4D5 protein expressions. Overall PDE4D expression was similar in control and patient cells, but the expression of PDE4D5 isoform was slightly higher in patient cells.

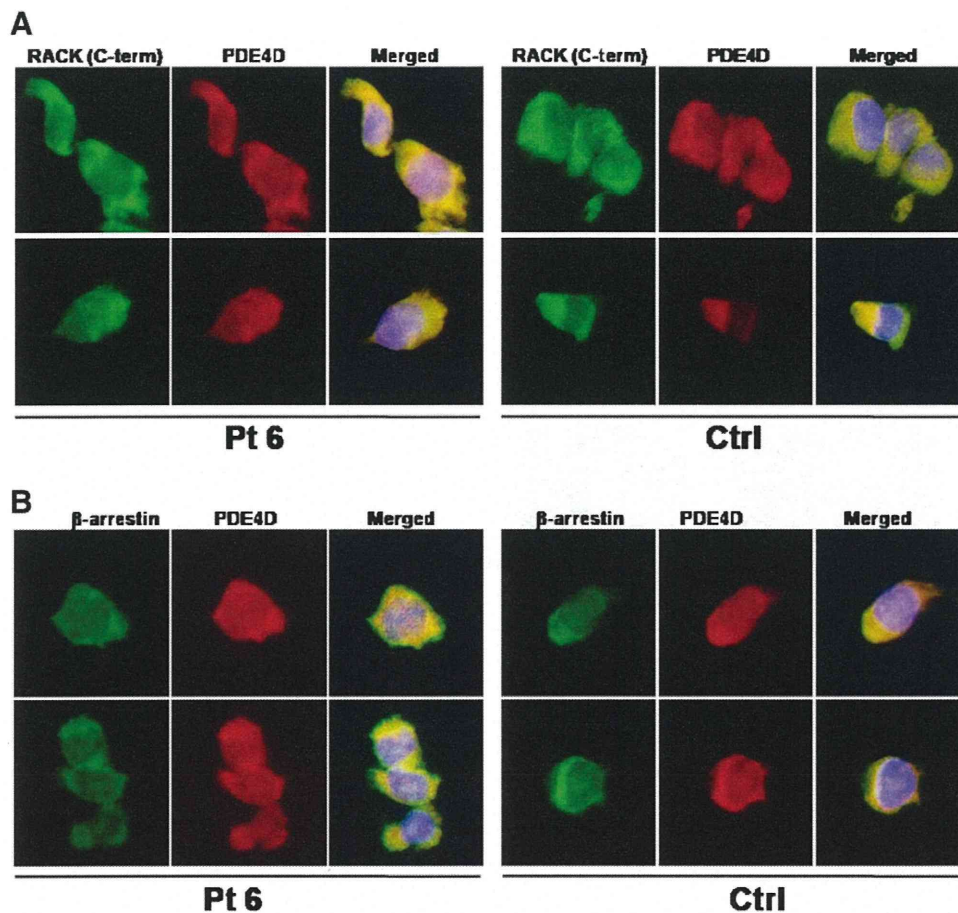


Fig. 5. Intracellular localization of PDE4D, RACK-1, and β -arrestin in EBV-transformed lymphocytes. Panel A shows the localization of PDE4D and RACK-1 in EBV-transformed lymphocytes. Immunofluorescent staining for RACK-1 and PDE4D were performed using rabbit anti-RACK-1 antibody and Alexa488-conjugated goat anti-rabbit IgG (left panel), and goat anti-PDE4D antibody and Alexa568-conjugated donkey anti-goat IgG (middle panel). Nuclei were counterstained with DAPI. Right panels show merged images of RACK-1 and PDE4D. Panel B shows the localization of PDE4D and β -arrestin in EBV-transformed lymphocytes. Immunofluorescent staining for beta-arrestin and PDE4D were performed using mouse anti- β -arrestin antibody and Alexa488-conjugated goat anti-mouse IgG (left panel), and goat anti-PDE4D antibody and Alexa568-conjugated donkey anti-goat IgG (middle panel). Nuclei were counterstained with DAPI. Right panels show merged images of β -arrestin and PDE4D. Colocalization of PDE4D and RACK-1 or β -arrestin was not different in cells from the patient and control subject.

PHP-1a (e.g., AHO) are accompanied by hormonal resistance. Remarkably, hormonal resistance is milder in patients with acrodysostosis caused by the *PRKARIA* mutation, and even this hormonal resistance is apparently lost in acrodysostosis caused by *PDE4D* mutation. Therefore, hormonal resistance and skeletal dysplasia may represent a spectrum of signal transduction pathway-associated disorders, at least for AHO and acrodysostosis. We suggest that pursuing gene discovery in these diseases should continue, especially in patients who show combined mild hormonal resistance and skeletal manifestations.

In silico 3D structure analyses and *in vitro* transfection assays, using mutants that reflected those seen in the patients (Figs. 2 and 3), predicted an increase in the cAMP level caused by decreased PDE4D activity. However, our functional analyses of cells from patients with a *PDE4D* mutation were contradictory to this in that, compared to cells from control subjects, we observed a reduced, rather than an enhanced cAMP accumulation in response to forskolin activation of adenylyl cyclase. However, we resolved the basis of this apparent discrepancy by showing that, in cells from acrodysostosis patients, there appeared to be an up-regulation of PDE4 isoforms from other sub-families whose activity over-compensated for the loss of PDE4D activity (Fig. 4). Thus chronic adaptation to a deficient PDE4D environment appears to foster the over-compensation of the expression of other PDE4 species that likely explains the decreased cAMP accumulation and decreased CREB phosphorylation, compared to cells from normal subjects, seen in cells

from acrodysostosis patients in response to forskolin challenge (Figs. 3 and 4). This parallels the situation where PKA activity is compromised by the *PRKARIA* mutation, as in acrodysostosis without hormone resistance, which may explain why patients with inactivating PDE4D mutations phenotypically show acrodysostosis. Thus, it seems that acrodysostosis patients who are chronically expressing catalytically compromised PDE4D from conception elicits an adaptive response that takes the form of up-regulation of isoforms from other PDE4 sub-families and that this overcompensates for the reduced activity caused by PDE4D mutation.

The myriad of 20 + PDE4 isoforms are believed to each have distinct, complex promoters but little, however, is known about their precise structure and regulation [65]. Nevertheless, previous studies on PDE4D5, PDE4A11, PDE4D1/2 has shown that they can confer both up- and down-regulation in response to altered cAMP levels [30–33, 66]. Thus analyses of the basis for the up-regulation of PDE4C, PDE4D5 and PDE4D11, which we observed in cells from acrodysostosis patients will require very considerable effort to resolve in future studies. Interestingly, however, there is a paucity of research that has been carried out on the PDE4C gene family and little is known about its precise functional significance, range of isoforms, regulation and distribution, except that it is poorly expressed in the brain [67,68]. However, we now know that an important consequence of PDE4 isoform diversity is that it allows the targeting of particular isoforms to specific signaling complexes,

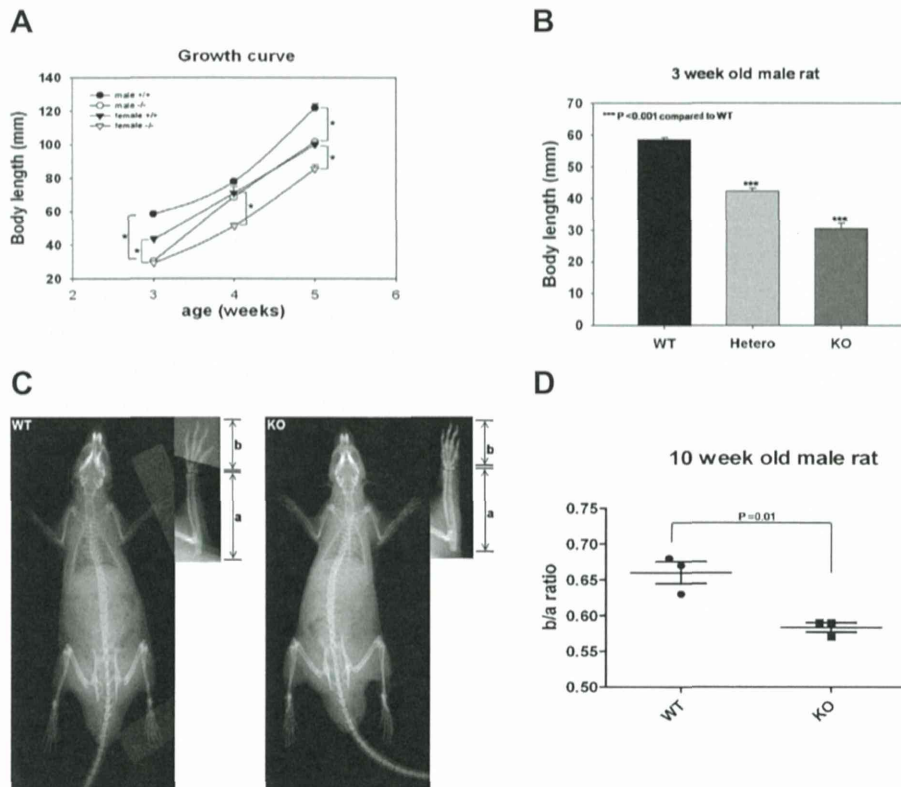


Fig. 6. Skeletal characteristics of PDE4D-KO rats. After birth, WT, heterozygous, and homozygous PDE4D-null rats were examined by measuring body length (nose-to-anus distance, N–A) using digital calipers. A. Starting from postnatal week 3, KO rats appeared significantly smaller than their control littermates. B. Male KO rats were significantly shorter than their WT and heterozygote littermates at 3 weeks. Data are shown as means \pm SEM. C and D. The b/a ratios of male KO rats were significantly lower than those of WT rats at 10 weeks. Decreased b/a ratios correspond to brachydactyly, which is seen in patients with acrodysostosis. (a: length of a forearm; b: length of a forepaw).

which allows them to exert distinct functional roles [18]. Thus, while up-regulation of PDE4C may compensate for a lowering of overall PDE4 activity due to chronic expression of the mutant PDE4D isoforms, PDE4C is unlikely to result in identical sequestration of the same signaling complexes in cells that would be seen with the various PDE4D isoforms. This ‘failure’ is likely to elicit an up-regulation of PDE4C to higher levels than to be seen with PDE4D, as the cell strives to generate enough active PDE4 to pair with the signaling complexes involving PDE4D. Additionally, the mass action effect due to the increased level of PDE4 isoform expression in acrodysostosis with hormone resistance patients is likely to cause increased sequestration of binding partners involving PDE4C and PDE4D5/11, which may itself lead to functional changes [7].

The patients with PDE4D mutations notably had no apparent hormone resistance, unlike the patients with PRKAR1A mutations [5]. Our patient 3, who harbored the PRKAR1A mutation, as well as three patients with the same mutation in the previous report, had hormone resistance. However, our patients with PDE4D mutations did not show any clinical evidence of hormone resistance. One possible explanation for the presence or absence of hormone resistance in PDE4D-related acrodysostosis is related to the extreme diversity of the PDE isoenzymes and their tissue-specific patterns of expression. In fact, PDE4 is one of the main isoenzymes in the osteoblast [69]. On the other hand, PRKAR1A is a common pathway gene in the Gs α -cAMP-PKA signal transduction pathway; therefore, mutation in this gene may cause acrodysostosis as well as hormone resistance [70]. Another possibility is that if the core acrodysostosis phenotype in PDE4D mutation patients is due to compensatory up-regulation of PDE4C, with concomitant down-regulation of PKA activity and CREB phosphorylation, then the lack of hormone resistance may be due to the lowered PDE4D activity. This can be expected to allow activation of a pool of PKA sequestered close to it, as we have

shown in ‘dominant negative’ approaches [21]. This would allow a key difference with PRKAR1A mutations, where all of the PKA-RI activity is compromised, to the PDE4D mutations where we propose that the major pool of PKA-RI activity will be compromised due to PDE4C up-regulation, while a PKA-RI pool associated with catalytically compromised PDE4D will be more active. Possibly, phosphorylation of a hormone receptor component associated with a PKA/PDE4D signaling complex negates hormone resistance in patients PDE4D mutations.

Finally, we tried to prove that loss of function of PDE4D in the long run results in the abnormalities of skeletal bone formation, as in human. In order to undertake this we employed a PDE4D knockout analysis using the rat, as mice are too small to discern the level of phenotypic change of KO expected. To address this hypothesis, we generated, for the first time, a KO of PDE4D in the rat; a larger rodent. In humans, skeletal manifestation of acrodysostosis without hormonal resistance consists of short stature, shortening of the distal part of the limb (especially the metacarpals and phalanges), and nasal bone hypoplasia. Nasal bone changes in the KO rat were difficult to discern. However, other manifestations in the bones were evident including significantly stunted growth in each gender at the age of 3 and 5 weeks. Moreover, this stunted growth was observed both in the KO rat and in heterozygote rats, as was it indeed noted in PDE4D deficient mice [71]. The most intriguing finding in this model was the observation that skeletal radiographs of 10-week-old KO rats showed shorter distal parts of the forelimbs (radius and palm) than in wild type rats and all of the metacarpals and phalanges of KO rat were also shorter than in the WT rat, as the name acrodysostosis implies. Our results show the strength of the KO rat model in terms of observing the relative bone change in the small bones.

It remains to be appreciated as to which specific PDE4D isoforms are critical to this pathology and whether mutations affect distinct isoform

differently. Certainly there is a growing appreciation that PDE4D isoforms perform distinct functional roles (see e.g. [21]) and can provide important regulatory enzymes that affect cell proliferation [72]) and the cell cycle [73].

5. Conclusions

In conclusion, as has been observed with GNAS and PRKAR1A, PDE4D serves as a key regulatory element in the cAMP signal transduction pathway and influences bone formation that leads to skeletal dysplasia. We propose that specific inhibitory PDE4D mutations provide the focus that triggers the molecular pathology of acrodysostosis without hormone resistance. However, we need to appreciate that aspects of the pathological phenotype may well also be dependent on an over-compensatory induction of other PDE4 isoforms that can be expected to be targeted to different signaling complexes and exert distinct effects on compartmentalized cAMP signaling.

Conflict of interest

All of the authors have no conflict of interest.

Acknowledgments

This study was supported by grants from the Korea Healthcare Technology R&D Project, Ministry for Health, Welfare and Family Affairs, Republic of Korea (A080588), the Samsung Biomedical Research Institute grant (SBRI C-A9-240-3), the Korea Science and Engineering Foundation (KOSEF) grant funded by the Korean government (MEST) (no. 2008-006198), Center for Clinical Research (PHO 1100931 Green Cross), and a grant from the Ministry of Health, Labour and Welfare, Japan (H23-Jitsuyoka(Nanbyo)-Ippan-007). We thank KIAS Center for Advanced Computation for providing the Linux cluster system for computational modeling.

References

- [1] L.C. Wilson, M.E. Oude Luttikhuis, M. Baraitser, H.M. Kingston, R.C. Trembath, *J. Med. Genet.* 34 (1997) 133–136.
- [2] M.G. Butler, L.J. Rames, W.B. Wadlington, *Am. J. Med. Genet.* 30 (1988) 971–980.
- [3] M.D. Houslay, G. Milligan, *Trends Biochem. Sci.* 22 (1997) 217–224.
- [4] J.M. Graham Jr., D. Krakow, V.T. Tolo, A.K. Smith, R.S. Lachman, *Pediatr. Radiol.* 31 (2001) 2–9.
- [5] A. Linglart, C. Menguy, A. Couvineau, C. Auzan, Y. Gunes, M. Cancel, E. Motte, G. Pinto, P. Chanson, P. Bougneres, E. Clauser, C. Silve, *N. Engl. J. Med.* 364 (2011) 2218–2226.
- [6] M. Breckler, M. Berthouze, A.C. Laurent, B. Crozatier, E. Morel, F. Lezoualc'h, *Cell. Signal.* 23 (2011) 1257–1266.
- [7] M.D. Houslay, *Trends Biochem. Sci.* 35 (2010) 91–100.
- [8] C. Lugnier, *Pharmacol. Ther.* 109 (2006) 366–398.
- [9] M.D. Houslay, P. Schafer, K.Y. Zhang, *Drug Discov. Today* 10 (2005) 1503–1519.
- [10] C.P. Page, D. Spina, *Curr. Opin. Pharmacol.* 12 (2012) 275–286.
- [11] C.P. Page, D. Spina, *Handb. Exp. Pharmacol.* (2011) 391–414.
- [12] B. Beghe, K.F. Rabe, L.M. Fabbri, *Am. J. Respir. Crit. Care Med.* 188 (2013) 271–278.
- [13] A. Hatzelmann, E.J. Morcillo, G. Lungarella, S. Adnot, S. Sanjar, R. Beume, C. Schudt, H. Tenor, *Pulm. Pharmacol. Ther.* 23 (2010) 235–256.
- [14] K.F. Rabe, *Br. J. Pharmacol.* 163 (2011) 53–67.
- [15] P.H. Schafer, R.M. Day, *J. Am. Acad. Dermatol.* 68 (2013) 1041–1042.
- [16] M. Wittmann, P.S. Helliwell, *Dermatol. Ther. (Heidelb)* 3 (2013) 1–15.
- [17] M. Conti, J. Beavo, *Annu. Rev. Biochem.* 76 (2007) 481–511.
- [18] T. Keravis, C. Lugnier, *Curr. Pharm. Des.* 16 (2010) 1114–1125.
- [19] M.D. Houslay, G.S. Baillie, D.H. Maurice, *Circ. Res.* 100 (2007) 950–966.
- [20] K. McCormick, G.S. Baillie, *Curr. Opin. Genet. Dev.* 27C (2014) 20–25.
- [21] A. McCahill, T. McSorley, E. Huston, E.V. Hill, M.J. Lynch, I. Gall, G. Keryer, B. Lygren, K. Tasken, G. van Heeke, M.D. Houslay, *Cell. Signal.* 17 (2005) 1158–1173.
- [22] G.B. Bolger, G.S. Baillie, X. Li, M.J. Lynch, P. Herzyk, A. Mohamed, L.H. Mitchell, A. McCahill, C. Hundsrucker, E. Klusmann, D.R. Adams, M.D. Houslay, *Biochem. J.* 398 (2006) 23–36.
- [23] G.S. Baillie, A. Sood, I. McPhee, I. Gall, S.J. Perry, R.J. Lefkowitz, M.D. Houslay, *Proc. Natl. Acad. Sci. U. S. A.* 100 (2003) 940–945.
- [24] A. Terrin, S. Monterisi, A. Stangherlin, A. Zoccarato, A. Koschinski, N.C. Surdo, M. Mongillo, A. Sawa, N.E. Jordanides, J.C. Mountford, M. Zaccolo, *J. Cell Biol.* 198 (2012) 607–621.
- [25] M.J. Lynch, G.S. Baillie, A. Mohamed, X. Li, C. Maisonneuve, E. Klusmann, G. van Heeke, M.D. Houslay, *J. Biol. Chem.* 280 (2005) 33178–33189.
- [26] Y. Shakur, J.G. Pryde, M.D. Houslay, *Biochem. J.* 292 (Pt 3) (1993) 677–686.
- [27] E. Huston, I. Gall, T.M. Houslay, M.D. Houslay, *J. Cell Sci.* 119 (2006) 3799–3810.
- [28] G.S. Baillie, E. Huston, G. Scotland, M. Hodgkin, I. Gall, A.H. Peden, C. MacKenzie, E.S. Houslay, R. Currie, T.R. Pettitt, A.R. Walmsley, M.J. Wakelam, J. Warwicker, M.D. Houslay, *J. Biol. Chem.* 277 (2002) 28298–28309.
- [29] M.J. Lynch, G.S. Baillie, M.D. Houslay, *Biochem. Soc. Trans.* 35 (2007) 938–941.
- [30] E. Vicini, M. Conti, *Mol. Endocrinol.* 11 (1997) 839–850.
- [31] I.R. Le Jeune, M. Shepherd, G. Van Heeke, M.D. Houslay, I.P. Hall, *J. Biol. Chem.* 277 (2002) 35980–35989.
- [32] D.A. Wallace, L.A. Johnston, E. Huston, D. MacMaster, T.M. Houslay, Y.F. Cheung, L. Campbell, J.E. Millen, R.A. Smith, I. Gall, R.G. Knowles, M. Sullivan, M.D. Houslay, *Mol. Pharmacol.* 67 (2005) 1920–1934.
- [33] A. McCahill, L. Campbell, T. McSorley, A. Sood, M.J. Lynch, X. Li, C. Yan, G.S. Baillie, M.D. Houslay, (PDE4A10), *Cell. Signal.* 20 (2008) 2071–2083.
- [34] G. Bolger, T. Michaeli, T. Martins, T. St John, B. Steiner, L. Rodgers, M. Riggs, M. Wigler, K. Ferguson, *Mol. Cell. Biol.* 13 (1993) 6558–6571.
- [35] C. Sette, M. Conti, *J. Biol. Chem.* 271 (1996) 16526–16534.
- [36] N. Okii, S.I. Takahashi, H. Hidaka, M. Conti, *J. Biol. Chem.* 275 (2000) 10831–10837.
- [37] D. Miika, W. Richter, R.E. Westenbroek, W.A. Catterall, M. Conti, *J. Cell Sci.* 127 (2014) 1033–1042.
- [38] D. Willoughby, G.S. Baillie, M.J. Lynch, A. Ciruela, M.D. Houslay, D.M. Cooper, *J. Biol. Chem.* 282 (2007) 34235–34249.
- [39] R. Hoffmann, I.R. Wilkinson, J.F. McCallum, P. Engels, M.D. Houslay, *Biochem. J.* 333 (Pt 1) (1998) 139–149.
- [40] M.B. Beard, A.E. Olsen, R.E. Jones, S. Erdogan, M.D. Houslay, G.B. Bolger, *J. Biol. Chem.* 275 (2000) 10349–10358.
- [41] S.J. MacKenzie, G.S. Baillie, I. McPhee, C. MacKenzie, R. Seamons, T. McSorley, J. Millen, M.B. Beard, G. van Heeke, M.D. Houslay, (UCR1), *Br. J. Pharmacol.* 136 (2002) 421–433.
- [42] D.M. Collins, H. Murdoch, A.J. Dunlop, E. Charych, G.S. Baillie, Q. Wang, F.W. Herberg, N. Brandon, A. Prinz, M.D. Houslay, (PDE4D3) in a manner that is dynamically regulated through Protein Kinase A (PKA), *Cell. Signal.* 20 (2008) 2356–2369.
- [43] K.F. MacKenzie, D.A. Wallace, E.V. Hill, D.F. Anthony, D.J. Henderson, D.M. Houslay, J. S. Arthur, G.S. Baillie, M.D. Houslay, *Biochem. J.* 435 (2011) 755–769.
- [44] N. Niikawa, I. Matsuda, T. Ohsawa, T. Kajii, *Hum. Genet.* 42 (1978) 227–232.
- [45] J.M. Ko, K.S. Kwack, S.-H. Kim, H.-J. Kim, *J. Genet. Med.* 7 (2010) 145–150.
- [46] E. Nii, M. Urawa, T. Nshimura, H. Kitou, S. Ikegawa, S. Shimizu, H. Taneda, A. Uchida, N. Niikawa, *Am. J. Med. Genet. B Neuro psychiatr. Genet.* 144B (2007) 824–825.
- [47] G.B. Bolger, S. Erdogan, R.E. Jones, K. Loughney, G. Scotland, R. Hoffmann, I. Wilkinson, C. Farrell, M.D. Houslay, *Biochem. J.* 328 (Pt 2) (1997) 539–548.
- [48] K. Joo, J. Lee, S. Lee, J.H. Seo, S.J. Lee, J. Lee, *Proteins* 69 (Suppl. 8) (2007) 83–89.
- [49] K. Joo, J. Lee, I. Kim, S.J. Lee, J. Lee, *Biophys. J.* 95 (2008) 4813–4819.
- [50] K. Joo, J. Lee, J.H. Seo, K. Lee, B.G. Kim, J. Lee, *Proteins* 75 (2009) 1010–1023.
- [51] M. Tress, J. Cheng, P. Baldi, K. Joo, J. Lee, J.H. Seo, J. Lee, D. Baker, D. Chivian, D. Kim, I. Ezkurdia, *Proteins* 69 (Suppl. 8) (2007) 137–151.
- [52] O. Trott, A.J. Olson, *J. Comput. Chem.* 31 (2010) 455–461.
- [53] B. Lu, A.M. Geurts, C. Poirier, D.C. Petit, W. Harrison, P.A. Overbeek, C.E. Bishop, *Mamm. Genome* 18 (2007) 338–346.
- [54] G.S. Baillie, *FEBS J.* 276 (2009) 1790–1799.
- [55] M.D. Houslay, D.R. Adams, *Biochem. J.* 370 (2003) 1–18.
- [56] K.J. Smith, G.S. Baillie, E.L. Hyde, X. Li, T.M. Houslay, A. McCahill, A.J. Dunlop, G.B. Bolger, E. Klusmann, D.R. Adams, M.D. Houslay, *Cell. Signal.* 19 (2007) 2612–2624.
- [57] H.V. Edwards, F. Christian, G.S. Baillie, *Semin. Cell Dev. Biol.* 23 (2012) 181–190.
- [58] B.E. Himes, G.M. Hunninghake, J.W. Baurley, N.M. Rafaels, P. Sleiman, D.P. Strachan, J. B. Wilk, S.A. Willis-Owen, B. Klanderman, J. Lasky-Su, R. Lazarus, A.J. Murphy, M.E. Soto-Cueros, L. Avila, T. Beaty, R.A. Mathias, I. Ruczinski, K.C. Barnes, J.C. Celedon, W.O. Cookson, W.J. Gauderman, F.D. Gilliland, H. Hakonarson, C. Lange, M.F. Moffatt, G.T. O'Connor, B.A. Raby, E.K. Silverman, S.T. Weiss, *Am. J. Hum. Genet.* 84 (2009) 581–593.
- [59] S. Shifman, A. Bhomra, S. Smiley, N.R. Wray, M.R. James, N.G. Martin, J.M. Hetttema, S.S. An, M.C. Neale, E.J. van den Oord, K.S. Kendler, X. Chen, D.I. Boomsma, C.M. Middeldorp, J.J. Hottenga, P.E. Slagboom, J. Flint, *Mol. Psychiatry* 13 (2008) 302–312.
- [60] S. Gretarsdottir, G. Thorleifsson, S.T. Reynisdottir, A. Manolescu, S. Jonsdottir, T. Jonsdottir, T. Gudmundsdottir, S.M. Bjarnadottir, O.B. Einarsson, H.M. Gudjonsson, M. Hawkins, G. Gudmundsson, H. Gudmundsdottir, H. Andrason, A.S. Gudmundsdottir, M. Sigurdardottir, T.T. Chou, J. Nahmias, S. Goss, S. Sveinbjornsdottir, E.M. Valdimarsson, F. Jakobsson, U. Agnarsson, V. Gudnason, G. Thorgeirsson, J. Fingerle, M. Gurney, D. Gudbjartsson, M.L. Frigge, A. Kong, K. Stefansson, J.R. Gulcher, *Nat. Genet.* 35 (2003) 131–138.
- [61] C. Wu, Z. Hu, Z. He, W. Jia, F. Wang, Y. Zhou, Z. Liu, Q. Zhan, Y. Liu, D. Yu, K. Zhai, J. Chang, Y. Qiao, G. Jin, Z. Liu, Y. Shen, C. Guo, J. Fu, X. Miao, W. Tan, H. Shen, Y. Ke, Y. Zeng, T. Wu, D. Lin, *Nat. Genet.* 43 (2011) 679–684.
- [62] C. Michot, C. Le Goff, A. Goldenberg, A. Abhyankar, C. Klein, E. Kinning, A.M. Guerrot, P. Flahaut, A. Duncombe, G. Baujat, S. Lyonnet, C. Thalassinou, P. Nitschke, J.L. Casanova, M. Le Merrer, A. Munnich, V. Cormier-Daire, *Am. J. Hum. Genet.* 90 (2012) 740–745.
- [63] H. Lee, J.M. Graham Jr., D.L. Rimoin, R.S. Lachman, P. Krejci, S.W. Tompson, S.F. Nelson, D. Krakow, D.H. Cohn, *Am. J. Hum. Genet.* 90 (2012) 746–751.
- [64] L.S. Kirschner, J.A. Carney, S.D. Pack, S.E. Taymans, C. Giatzakis, Y.S. Cho, Y.S. Cho-Chung, C.A. Stratakis, *Nat. Genet.* 26 (2000) 89–92.
- [65] M.D. Houslay, *Prog. Nucleic Acid Res. Mol. Biol.* 69 (2001) 249–315.

- [66] G. Rena, F. Begg, A. Ross, C. MacKenzie, I. McPhee, L. Campbell, E. Huston, M. Sullivan, M.D. Houslay, *Mol. Pharmacol.* 59 (2001) 996–1011.
- [67] M. Sullivan, A.S. Olsen, M.D. Houslay, *Cell. Signal.* 11 (1999) 735–742.
- [68] R.J. Owens, S. Lumb, K. Rees-Milton, A. Russell, D. Baldock, V. Lang, T. Crabbe, M. Ballesteros, M.J. Perry, *Cell. Signal.* 9 (1997) 575–585.
- [69] S. Wakabayashi, T. Tsutsumimoto, S. Kawasaki, T. Kinoshita, H. Horiuchi, K. Takaoka, *J. Bone Miner. Res.* 17 (2002) 249–256.
- [70] S.R. Neves, P.T. Ram, R. Iyengar, *Science* 296 (2002) 1636–1639.
- [71] S.L. Jin, F.J. Richard, W.P. Kuo, A.J. D'Ercole, M. Conti, *Proc. Natl. Acad. Sci. U. S. A.* 96 (1999) 11998–12003.
- [72] D.J. Henderson, A. Byrne, K. Dulla, G. Jenster, R. Hoffmann, G.S. Baillie, M.D. Houslay, *Br. J. Cancer* 110 (2014) 1278–1287.
- [73] C.L. Sheppard, L.C. Lee, E.V. Hill, D.J. Henderson, D.F. Anthony, D.M. Houslay, K.C. Yalla, L.S. Cairns, A.J. Dunlop, G.S. Baillie, E. Huston, M.D. Houslay, *Cell. Signal.* 26 (2014) 1958–1974.

RESEARCH

Open Access

Japanese founder duplications/triplications involving *BHLHA9* are associated with split-hand/foot malformation with or without long bone deficiency and Gollop-Wolfgang complex

Eiko Nagata^{1†}, Hiroki Kano^{2†}, Fumiko Kato¹, Rie Yamaguchi¹, Shinichi Nakashima¹, Shinichiro Takayama³, Rika Kosaki⁴, Hidefumi Tonoki⁵, Seiji Mizuno⁶, Satoshi Watanabe⁷, Koh-ichiro Yoshiura⁷, Tomoki Kosho⁸, Tomonobu Hasegawa⁹, Mamori Kimizuka¹⁰, Atsushi Suzuki¹¹, Kenji Shimizu¹¹, Hirofumi Ohashi¹¹, Nobuhiko Haga¹², Hironao Numabe¹³, Emiko Horii¹⁴, Toshiro Nagai¹⁵, Hiroshi Yoshihashi¹⁶, Gen Nishimura¹⁷, Tatsushi Toda¹⁸, Shuji Takada¹⁹, Shigetoshi Yokoyama^{19,22}, Hiroshi Asahara^{19,20}, Shinichiro Sano^{1,21}, Maki Fukami²¹, Shiro Ikegawa² and Tsutomu Ogata^{1*}

Abstract

Background: Limb malformations are rare disorders with high genetic heterogeneity. Although multiple genes/loci have been identified in limb malformations, underlying genetic factors still remain to be determined in most patients.

Methods: This study consisted of 51 Japanese families with split-hand/foot malformation (SHFM), SHFM with long bone deficiency (SHFLD) usually affecting the tibia, or Gollop-Wolfgang complex (GWC) characterized by SHFM and femoral bifurcation. Genetic studies included genomewide array comparative genomic hybridization and exome sequencing, together with standard molecular analyses.

Results: We identified duplications/triplications of a 210,050 bp segment containing *BHLHA9* in 29 SHFM patients, 11 SHFLD patients, two GWC patients, and 22 clinically normal relatives from 27 of the 51 families examined, as well as in 2 of 1,000 Japanese controls. Families with SHFLD- and/or GWC-positive patients were more frequent in triplications than in duplications. The fusion point was identical in all the duplications/triplications and was associated with a 4 bp microhomology. There was no sequence homology around the two breakpoints, whereas rearrangement-associated motifs were abundant around one breakpoint. The rs3951819-D17S1174 haplotype patterns were variable on the duplicated/triplicated segments. No discernible genetic alteration specific to patients was detected within or around *BHLHA9*, in the known causative SHFM genes, or in the exome.

(Continued on next page)

* Correspondence: tomogata@hama-med.ac.jp

†Equal contributors

¹Department of Pediatrics, Hamamatsu University School of Medicine, Hamamatsu 431-3192, Japan

Full list of author information is available at the end of the article

(Continued from previous page)

Conclusions: These results indicate that *BHLHA9* overdosage constitutes the most frequent susceptibility factor, with a dosage effect, for a range of limb malformations at least in Japan. Notably, this is the first study revealing the underlying genetic factor for the development of GWC, and demonstrating the presence of triplications involving *BHLHA9*. It is inferred that a Japanese founder duplication was generated through a replication-based mechanism and underwent subsequent triplication and haplotype modification through recombination-based mechanisms, and that the duplications/triplications with various haplotypes were widely spread in Japan primarily via clinically normal carriers and identified via manifesting patients. Furthermore, genotype-phenotype analyses of patients reported in this study and the previous studies imply that clinical variability is ascribed to multiple factors including the size of duplications/triplications as a critical factor.

Keywords: *BHLHA9*, Split-hand/foot malformation, Long bone deficiency, Gollop-Wolfgang complex, Expressivity, Penetrance, Susceptibility, Japanese founder copy number gain

Introduction

Split-hand/foot malformation (SHFM), also known as ectrodactyly, is a rare limb malformation involving the central rays of the autopod [1,2]. It presents with median clefts of the hands and feet, aplasia/hypoplasia of the phalanges, metacarpals, and metatarsals, and syndactyly. SHFM results from failure to maintain the central portion of the apical ectodermal ridge (AER) in the developing autopod [1,2]. SHFM is divided into two forms: a non-syndromic form with limb-confined manifestations and a syndromic form with extra-limb manifestations [2]. Furthermore, non-syndromic SHFM can occur as an isolated abnormality confined to digits (hereafter, SHFM refers to this type) or in association with other limb abnormalities as observed in SHFM with long bone deficiency (SHFLD) usually affecting the tibia and in Gollop-Wolfgang complex (GWC) characterized by femoral bifurcation [1,2]. Both syndromic and non-syndromic forms are associated with wide expressivity and penetrance even among members of a single family and among limbs of a single patient [2].

SHFM and SHFLD are genetically heterogeneous conditions reviewed in ref. [2]. To date, SHFM has been identified in patients with heterozygous deletions or translocations involving the *DLX5-DLX6* locus at 7q21.2–21.3 (SHFM1) [3] (*DLX5* mutations have been detected recently), heterozygous duplications at 10q24 (SHFM3), heterozygous mutations of *TP63* at 3q27 (SHFM4), heterozygous deletions affecting *HOXD* cluster at 2q31 (SHFM5), and biallelic mutations of *WNT10B* at 12q31 (SHFM6); in addition, SHFM2 has been assigned to Xq26 by linkage analyses in a large Pakistani kindred [2]. Similarly, a genomewide linkage analysis in a large consanguineous family has identified two SHFLD susceptibility loci, one at 1q42.2–q43 (SHFLD1) and the other at 6q14.1 (SHFLD2); furthermore, after assignment of another SHFLD locus to 17p13.1–13.3 [4], duplications at 17p13.3 (SHFLD3) have been found in patients with SHFLD reviewed in ref. [2]. However, the GWC locus (loci) remains unknown at present.

The duplications at 17p13.3 identified to date are highly variable in size, and harbor *BHLHA9* as the sole gene within the smallest region of overlap [5–9]. *Bhlha9/bhlha9* is expressed in the limb bud mesenchyme underlying the AER in mouse and zebrafish embryos, and *bhlha9* knockdown has resulted in shortening of the pectoral fins in zebrafish [6]. Furthermore, *BHLHA9*-containing duplications have been identified not only in patients with SHFLD but also in those with SHFM and clinically normal family members [4–10]. These findings argue for a critical role of *BHLHA9* duplication in the development of SHFM and SHFLD, with variable expressivity and incomplete penetrance.

In this study, we report on *BHLHA9*-containing duplications/triplications with an identical fusion point and various haplotype patterns that were associated with a range of limb malformations including GWC, and discuss on characteristic clinical findings, genomic basis of Japanese founder copy number gains, and underlying factors for phenotypic variability.

Materials and methods

Patients/subjects

We studied 68 patients with SHFM ($n = 55$), SHFLD ($n = 11$), or GWC ($n = 2$), as well as 60 clinically normal relatives, from 51 Japanese families; the pedigrees of 27 of the 51 families and representative clinical findings are shown in Figure 1. All the probands 1–51 had a normal karyotype. Southern blot analysis for SHFM3 locus had been performed in 28 probands with SHFM, indicating 10q24 duplications in two of them [11]. Clinical features including photographs and roentgenograms of a proband with GWC and his brother with SHFLD (family 23 in Figure 1A) were as described previously [12]. The residencies of families 1–51 were widely distributed throughout Japan.

Ethical approval and samples

This study was approved by the Institutional Review Board Committees of Hamamatsu University School of

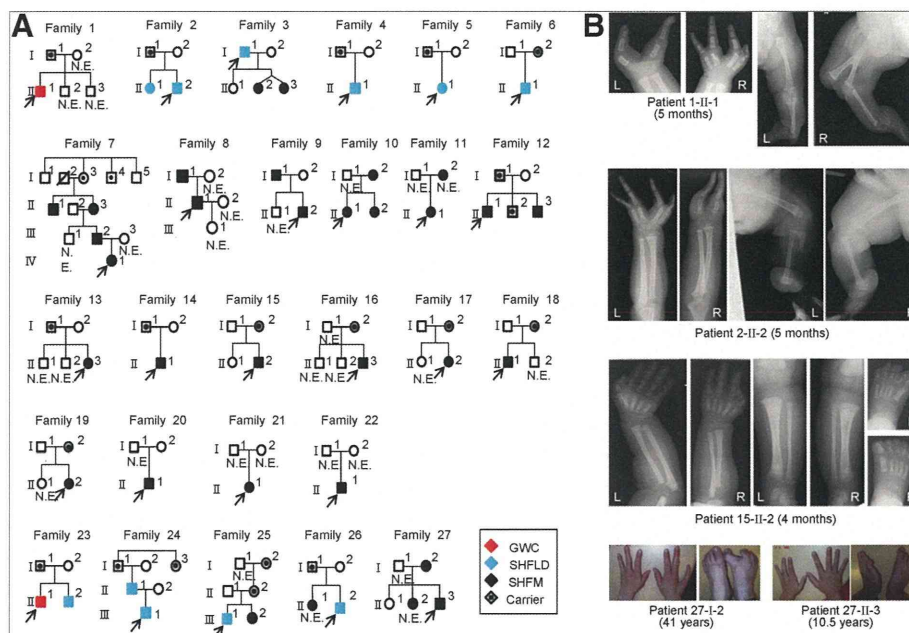


Figure 1 Clinical summary. **A.** Pedigrees of 27 Japanese families with duplications (families 1–22) and triplications (families 23–27) of a ~200 kb region involving *BHLHA9*. The duplications/triplications are associated with GWC, SHFLD, SHFM, or normal phenotype (carriers). N.E.: Not examined molecularly. **B.** Representative clinical findings. Each patient is indicated by a family-generation-individual style and corresponds to the patient/subject shown in Figure 1A and Additional file 5. The top panel: GWC with right bifid femur; the second panel: SHFLD with bilateral tibial deficiencies, the third panel: SHFM with polydactyly; and the bottom panel: SHFM.

Medicine, RIKEN, and National Center for Child Health and Development, and was performed using peripheral leukocyte samples after obtaining written informed consent for the molecular analysis and the publication of genetic and clinical data after removing information for personal identification (e.g., name, birthday, and facial photograph) from the adult subjects (³ 20 years) or from the parents of the child subjects (below 20 years). Furthermore, informed assent was also obtained from child subjects between 6–20 years.

Samples and primers

The primers utilized in this study are summarized in Additional file 1.

Molecular studies

Sanger sequencing, fluorescence *in situ* hybridization (FISH), microsatellite genotyping, Southern blotting, and bisulfite sequencing-based methylation analysis were performed by the standard methods, as reported previously [13]. Quantitative real-time PCR (qPCR) analysis was carried out by the SYBR Green methods on StepOnePlus system, using *RNaseP* as an internal control (Life Technologies). Genomewide oligonucleotide-based array comparative genomic hybridization (CGH) was performed with a catalog human array (4 × 180 K format, ID G4449A) according to the manufacturer's instructions (Agilent Technologies),

and obtained copy number variants/polymorphisms were screened with Agilent Genomic Workbench software using the Database of Genomic Variants (<http://dgv.tcag.ca/dgv/app/home>). Sequencing of a long region encompassing *BHLHA9* was performed with the Nextera XT kit on MiSeq (Illumina), using SAMtools v0.1.17 software (<http://samtools.sourceforge.net/>). Exome sequencing was performed as described previously [14].

Assessment of genomic environments around the fusion points

Repeat elements around the fusion point were searched for using Repeatmasker (<http://www.repeatmasker.org>). Rearrangement-inducing DNA features were investigated for 300 bp regions at both the proximal and the distal sides of each breakpoint, using GEECEE (<http://emboss.bioinformatics.nl/cgi-bin/emboss/geecee>) for calculation of the average GC content, PALINDROME (<http://mobyle.pasteur.fr/cgi-bin/portal.py#forms::palindrome>) and Non-B DB (<http://nonb.abcc.ncifcrf.gov>) for the examination of the palindromes and non-B (non-canonical) structures, and Fuzznuc (<http://emboss.bioinformatics.nl/cgi-bin/emboss/fuzznuc>) for the assessment of rearrangement-associated sequence motifs and tri/tetranucleotides [15-20]. For controls, we examined 48 regions of 600 bp long selected at an interval of 1.5 Mb from the entire chromosome 17.

Statistical analysis

The statistical significance of the frequency was analyzed by the two-sided Fisher's exact probability test.

Results

Sequence analysis of the known causative/candidate genes

We performed direct sequencing for the previously known causative genes (*DLX5*, *TP63*, and *WNT10B*) reviewed in ref. [2] in the probands 1–51. Although no pathologic mutation was identified in *DLX5* and *TP63*, the previously reported homozygous missense mutation of *WNT10B* (c.944C > T, p.R332W) [21] was detected in the proband 48 with SHFM who was born to healthy consanguineous parents heterozygous for this mutation. In addition, while no variation was detected in *DLX5* and *WNT10B*, rs34201045 (4 bp insertion polymorphism) in *TP63* [21] was detected with an allele frequency of 61%.

We also examined *BHLHA9*, because gain-of-function mutations of *BHLHA9* as well as *BHLHA9*-harboring duplications may lead to limb malformations. No sequence variation was identified in the 51 probands.

Array CGH analysis

Array CGH analysis was performed for the probands 1–51, showing increased copy numbers at 17p13.3 encompassing *BHLHA9* (SHFLD3) in the probands 1–27 from families 1–27 (Figure 1A). Furthermore, heterozygous duplications at 10q24 (SHFM3) were detected in the probands 49–51, i.e., a hitherto unreported patient with paternally inherited SHFM (his father also had the duplication) and the two patients who had been indicated to have the duplications by Southern blot analysis [11]. No copy number alteration was observed at other SHFM/SHFLD loci in the probands 1–27 and 49–51. In the remaining probands 28–48, there was no copy number variation that was not registered in the Database of Genomic Variants.

Identical fusion points in *BHLHA9*-containing duplications/triplications

The array CGH indicated that the increased copy number regions at 17p13.3 were quite similar in the physical size in the probands 1–27 and present in three copies in the probands 1–22 and in four copies in the probands 23–27 (Figure 2A). Thus, FISH analysis was performed using 8,259 bp PCR products amplified from this region, showing two signals with a different intensity that was more obvious in the probands 23–27 (Figure 2A).

We next determined the fusion points of the duplications/triplications (Figure 2B). PCR products of 2,195 bp long were obtained with P1/P2 primers in the probands 1–27, and the fusion point was determined by direct sequencing for 418 bp PCR products obtained with P3/P4

primers. The fusion point was identical in all the probands 1–27; it resided on intron 1 of *ABR* and intron 1 of *YWHAE*, and was associated with a 4 bp microhomology.

Then, we performed qPCR analysis for a 214 bp region harboring the fusion point, using P5/P6 primers (Figure 2C and Additional file 2). The fusion point was present in a single copy in the probands 1–22 and in two copies in the probands 23–27. The results showed that the identical genomic segment harboring *BHLHA9* was tandemly duplicated in the probands 1–22 and triplicated in the probands 23–27. According to GRCh37/hg19 (<http://genome.ucsc.edu/>), the genomic segment was 210,050 bp long.

We also performed array CGH and qPCR for the fusion point in 15 patients other than the probands and 47 clinically normal relatives from the 27 families (Figures 1 and 2C). The duplications/triplications were identified in all the 15 patients. Thus, in a total of 42 patients, duplications/triplications were found in 29 SHFM patients, 11 SHFLD patients, and two GWC patients. Furthermore, the duplications/triplications were also present in 22 of the 47 clinically normal relatives. In particular, they were invariably identified in either of the clinically normal parents when both of them were examined; they were also present in other clinically normal relatives in families 7, 12, 24, and 25.

Since the above data indicated the presence of duplications/triplications in clinically normal subjects, we performed qPCR for the fusion point in 1,000 Japanese controls. The fusion point was detected in a single copy in two subjects (Subjects 1 and 2 in Figure 2C). We also performed array CGH in 200 of the 1,000 controls including the two subjects, confirming the duplications in the two subjects and lack of other copy number variations, including deletions involving *BHLHA9*, which were not registered in the Database of Genomic Variants in the 200 control subjects. The frequency of duplications/triplications was significantly higher in the probands than in the control subjects (27/51 vs. 2/1,000, $P = 3.5 \times 10^{-37}$).

Various haplotype patterns on the duplicated/triplicated segments

We carried out genotyping for rs3951819 (A/G SNP on *BHLHA9*) and *D17S1174* (CA repeat microsatellite locus) on the genomic segment subjected to duplications/triplications (Figure 2A), and determined rs3951819-*D17S1174* haplotype patterns. Representative results are shown in Figure 2D, and all the data are available on request. Various haplotype patterns were identified on the single, the duplicated, and the triplicated segments, and the [A-14] haplotype was most prevalent on the duplicated/triplicated segments (Table 1). While the distribution of CA repeat lengths on the single segments was discontinuous, similar discontinuous distribution was

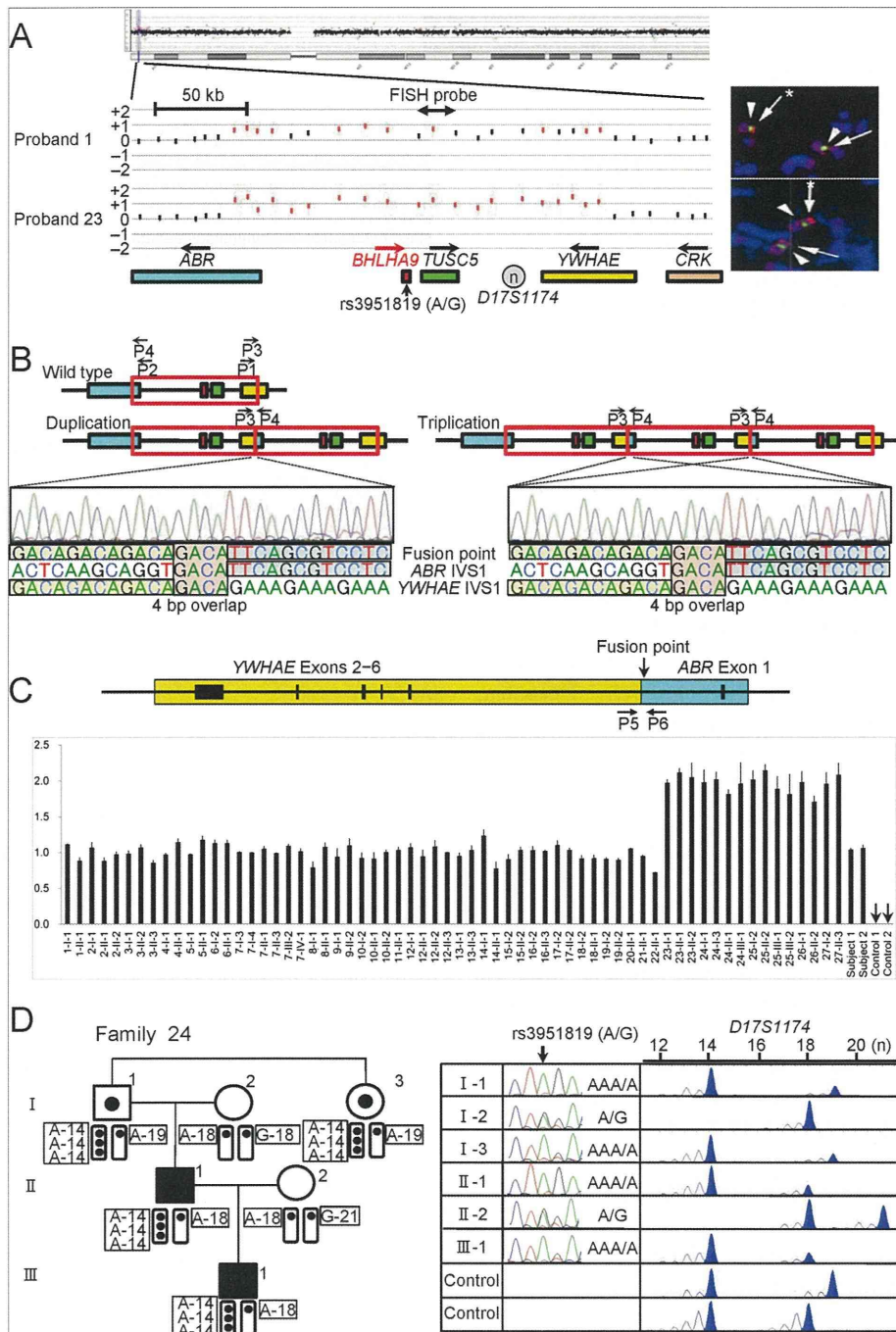


Figure 2 (See legend on next page.)

(See figure on previous page.)

Figure 2 Identification and characterization of the duplications/triplications involving *BHLHA9* at chromosome 17p13.3. **A.** Array CGH and FISH analyses in proband 1 and proband 23 with GWC. In array CGH analysis, the black and the red dots denote the normal and the increased copy numbers, respectively. Since the log₂ signal ratios for a ~200 kb region encompassing *BHLHA9* are around +0.5 in the proband 1 and around +1.0 in the proband 23, this indicates the presence of three and four copies of this region in the two probands, respectively. In FISH analysis, two red signals with an apparently different density are detected by the 8,289 bp PCR probe (the stronger signals are indicated with asterisks). The green signals derive from an internal control probe (CEP17). The arrows on the genes show transcriptional directions. Rs3951819 (A/G) resides within *BHLHA9*. **B.** Determination of the fusion point. The fusion has occurred between intron 1 of *ABR* and intron 1 of *YWHAE*, and is associated with a 4 bp (GACA) microhomology. P1–P4 show the position of primers. **C.** Quantitative real-time PCR analysis. The upper part denotes the fusion point. P5 & P6 show the position of primers. The lower part shows the copy number of the fusion point in patients/subjects with duplications/triplications (indicated by a family-generation-individual style corresponding to that in Figure 1 and Additional file 5). Subject-1 and subject-2 denote the two control subjects with the duplication, and control-1 and control-2 represent normal subjects without the duplication/triplication. **D.** The rs3951819 (A/G SNP)–*D17S1174* (CA repeat number) haplotype patterns in family 24. Assuming no recombination between rs3951819 and *D17S1174*, the haplotype patterns of the family members are determined as shown here. The haplotype patterns of the remaining families have been interpreted similarly.

also observed in the Japanese general population (see Additional file 3).

Genomic environments around the breakpoints

The breakpoint on *YWHAE* intron 1 resided on a simple *Alu* repeat sequence, and that on *ABR* intron 1 was present on a non-repetitive sequence. There was no low copy repeat around the breakpoints. Comparison of the frequencies of known rearrangement-inducing DNA features between 600 bp sequences around the breakpoints and those of 48 regions selected at an interval of 1.5 Mb from chromosome 17 revealed that palindromes, several types of non-B DNA structures, and a rearrangement-associated sequence motif were abundant around the breakpoint on *YWHAE* intron 1 (see Additional file 4).

Clinical findings of families 1–27

Clinical assessment revealed several notable findings. First, duplications/triplications were associated with SHFM, SHFLD, GWC, or normal phenotype, with inter- and intra-familial clinical variability (Figure 1A). Second, in the 42 patients, split hand (SH) was more prevalent than split foot (SF) (41/42 vs. 17/42, $P = 6.2 \times 10^{-9}$), and long bone defect (LBD) was confined to lower extremities (0/42 vs. 13/42, $P = 4.1 \times 10^{-5}$) (Table 2 and Additional file 5). Third, there was no significant sex difference in the ratio between patients with limb malformations and patients/carriers with duplications/triplications (26/38 in males vs. 16/26 in females, $P = 0.60$) (Table 2 and Additional file 5). Fourth, the ratio of LBD positive families was significantly higher in triplications than in duplications (4/5 vs. 16/22, $P = 0.047$) (Figure 1A and Table 2). Fifth, while the duplications/triplications were transmitted from patients to patients, from carriers to patients, and from a carrier to a carrier (from I-1 to II-2 in family 12), transmission from a patient to a carrier was not identified (Figure 1A); it should be pointed out, however, that molecular analysis in a clinically normal child born to an affected parent was possible only in a single adult subject (II-1 in family 27), and that molecular analysis in clinically

Table 1 The rs3951819 (A/G SNP) – *D17S1174* (CA repeat number) haplotype

Patterns of the 210,050 bp segment subjected to copy number gains	
Haplotype pattern	Family
<Single segment>	
[A-14]	1, 5, 9, 15, 17, 19, 23, 26
[A-16]	12
[A-18]	3, 14, 15, 24, 25, 26
[A-19]	2, 6, 13, 19, 20, 24, 25, 27
[A-21]	5, 23
[G-12]	17
[G-14]	2, 3, 6, 12, 13, 19, 26
[G-18]	3, 5, 17, 18, 24, 25
[G-19]	9, 12, 18, 20, 25
[G-21]	1, 9, 19, 24, 27
[A-14] or [G-14]	16
[A-18] or [G-18]	4
[A-19] or [G-19]	4
[A-21] or [G-21]	16
<Duplicated segments>	
[A-14] + [A-14]	5, 12, 13, 14, 15, 20
[A-14] + [A-18]	1
[A-14] + [G-18] or [G-14] + [A-18]	2, 3, 4, 6, 9, 16, 17
[A-14] + [G-18] or [A-14] + [G-19]	18
[A-14] + [G-14] or [G-14] + [G-14]	19
<Tripllicated segments>	
[A-14] + [A-14] + [A-14]	23, 24
[A-14] + [A-14] + [G-14]	25
[A-14] + [A-19] + [A-19]	26
[A-14] + [G-18] + [G-18] or [G-14] + [A-18] + [G-18]	27

The haplotype patterns written in the left column have been detected in at least one patient/subject in the families described in the right column. Genotyping could not be performed in several patients/subjects who had been repeatedly examined previously, because of the extremely small amount of DNA samples that were virtually used up in the sequencing and array CGH analyses.

Table 2 Summary of clinical findings in patients/carriers with duplications/triplications involving *BHLHA9*

	SHFM (+) patients			LBD (+) patients			Patient ratio*			LBD (+) families		
	SH	SF	P-value	U-LBD	L-LBD	P-value	Male	Female	P-value	Trip	Dup	P-value
This study	41/42	17/42	6.2×10^{-9}	0/42	13/42	4.1×10^{-5}	26/38	16/26	0.60	4/5	16/22	0.047
Previous studies	63/84	23/84	8.6×10^{-10}	11/91	42/91	5.7×10^{-7}	68/114	31/79	5.7×10^{-3}
Sum	104/126	40/126	1.1×10^{-16}	11/133	55/133	3.0×10^{-10}	94/152	47/105	7.6×10^{-3}

SHFM: split-hand/foot malformation; SH: split hand; SF: split foot; LBD: long bone deficiency; U: upper; L: lower; Trip: triplication; and Dup: duplication. In the previous studies, patients without detailed phenotypic description and those of unknown sex have been excluded (3–9).

*The ratio between patients with limb malformations and patients/carriers with duplications/triplications, i.e. the number of patients over the number of patients plus carriers.

normal children <20 years old was possible only in two subjects (II-2 in family 12 and II-1 in family 15). Lastly, limb malformation was inherited in an apparently autosomal dominant manner (from patients to patients), or took place as an apparently *de novo* event or as an apparently autosomal recessive trait (from clinically normal parents to a single or two affected children) (Figure 1A).

Attempts to identify a possible modifier(s)

The variable expressivity and incomplete penetrance in families 1–27 suggest the presence of a possible modifier (s) for the development of limb malformations. Thus, we performed further molecular studies in patients/subjects in whom DNA samples were still available, and compared the molecular data between patients with SHFM and those with SHFLD for the assessment of variable expressivity and between SHFM, SHFLD, or total patients and carriers for the evaluation of incomplete penetrance.

We first examined the possibility that the modifier(s) resides within or around *BHLHA9* (see Additional file 6). There was no *BHLHA9* mutation in all the 21 examined probands with SHFM, SHFLD, or GWC, as described in the section of “Sequence analysis of the known causative/candidate genes”. The rs3951819 A/G SNP pattern on the duplicated/triplicated segments was apparently identical between patients and carriers (e.g. Figure 2D), and the frequency of A/G allele on the normal chromosome 17 was similar between SHFM and SHFLD patients and between SHFM, SHFLD, or total patients and carriers (see Additional file 7). The results of other known SNPs on *BHLHA9* (rs185242872, rs18936498, and rs140504068) were not informative, because of absence or extreme rarity of minor alleles. Furthermore, in SHFM families 7, 12, and 18, sequencing of a 7,406 bp region encompassing *BHLHA9* and Southern blot analysis using five probes and *MfeI*-, *SspI*-, and *SacI*-digested genomic DNA revealed no variation specific to the patients, and methylation analysis for a CpG rich region at the upstream of *BHLHA9* delineated massive hypomethylation in all the patients/carriers examined.

Next, we examined the possibility that a variant(s) of known causative genes constitutes the modifier(s). Since rs34201045 in *TP63* was identified in the mutation

analysis, we compared rs34201045 genotyping data between the 27 probands and the 15 carriers. The allele and genotype frequencies were similar between SHFM and SHFLD patients and between SHFM, SHFLD, or total patients and carriers (see Additional file 8).

We finally performed exome sequencing in SHFM families 13 and 17–19. However, there was no variation specific to the patients. In addition, re-examination of the genomewide array CGH data showed no discernible copy number variation specific to the patients.

Discussion

BHLHA9 overdosage and clinical characteristics

We identified duplications/triplications of a ~200 kb genomic segment involving *BHLHA9* at 17p13.3 in 27 of 51 families with SHFM, SHFLD, or GWC. To our knowledge, this is the first study revealing the underlying genetic factor for the development of GWC, and demonstrating the presence of triplications involving *BHLHA9* that were suggested but not confirmed in the previous studies [5,9]. Furthermore, this study indicates that *BHLHA9*-containing duplications/triplications are the most frequent underlying factor for the development of limb malformations at least in Japan. Notably, SHFLD and GWC with LBD were significantly more frequent in patients with triplications than in those with duplications, and the duplications/triplications were identified in clinically normal familial members and in the general population. These findings imply that increased *BHLHA9* copy number constitutes a strong susceptibility, rather than a causative, factor with a dosage effect for the development of a range of limb malformations. Since *Bhlha9* is expressed in the developing ectoderm adjacent to the AER rather than the AER itself in mouse embryos [6], *BHLHA9* appears to play a critical role in the limb development by interacting with the AER. While the duplications/triplications identified in this study included *TUSC5* and generated an *ABR-YWHAE* chimeric gene (Figure 2C), *TUSC5* duplication and the chimeric gene formation are not common findings in the previously reported patients with duplications at 17p13.3 and SHFM and/or SHFLD [5–9]. In addition, none of *Tusc5*, *Abr*, and *Ywhae* is specifically expressed in the developing mouse limb buds [22] (A Transcriptome Atlas Database

for Mouse Embryo of Eurexpress Project, <http://www.eurexpress.org/ee/project/>).

Several clinical findings are noteworthy in patients/subjects with duplications/triplications. First, SH was more frequent than SF in this study as well as in the previous studies, and LBD was confined to lower extremities in this study and was more frequent in lower extremities than in upper extremities in the previous studies (Table 2) [4-10]. This implies that *BHLHA9* overdosage exerts differential effects on the different parts of limbs. Second, while limb malformations were similarly identified between males and females in this study, they were more frequently observed in males than in females in the previous studies (Table 2) [4-10]. In this regard, it has been reported that testosterone influences the digital growth pattern as indicated by the lower second to fourth digit length ratio in males than in females [23-25], and that Caucasian males have higher serum testosterone values and lower second to fourth digit length ratios than Oriental males [26,27]. Such testosterone effects on the digital growth pattern with ethnic difference may explain why male dominant manifestation was observed in the previous studies primarily from Caucasian countries and was not found in this study. Lastly, LBD was more prevalent in patients with triplications than in those with duplications. This suggests that LBD primarily occurs when the effects of *BHLHA9* overdosage are considerably elevated.

Genomic basis of the Japanese founder copy number gains

The duplications/triplications were associated with the same fusion point and variable haplotype patterns. Since there was no sequence homology or low-copy repeats around the breakpoints, it is unlikely that such duplications/triplications were recurrently produced in different individuals by non-allelic homologous recombination (NAHR) [17,20]. Instead, it is assumed that a Japanese founder duplication took place in a single ancestor, and was spread with subsequent triplication and modification of the haplotype patterns.

The most likely genomic basis of the Japanese duplications/triplications is illustrated in Additional file 9. Notably, a 4 bp (GACA) microhomology was identified at the duplication fusion point (Figure 2B). A microhomology refers to two to five nucleotides common to the sequences of the two breakpoints, and is found as an overlapping sequence at the join point [16,19,20]. This suggests that the Japanese founder duplication was generated by replication-based mechanisms such as fork stalling and template switching (FoSTeS) and microhomology-mediated break-induced replication (MMBIR), because the presence of such a microhomology is characteristic of FoSTeS/MMBIR [17-20]. Indeed, such a simple tandem duplication with a microhomology can be produced by one time FoSTeS/

MMBIR [17-20], although it could also be generated by non-homologous end-joining (NHEJ) [17]. Since the [A-14] haplotype was most prevalent on the duplicated/triplicated segments, it is inferred that a genomic rearrangement occurred in an ancestor with the [A-14] haplotype, yielding the founder duplication with the [A-14] + [A-14] haplotype. Furthermore, the presence of multiple stimulants for genomic rearrangements around the breakpoint on *YWHAE* intron 1 would have facilitated the generation of the founder duplication. In particular, non-B structures are known to stimulate the occurrence of both replication-based FoSTeS/MMBIR and double-strand breaks and resultant NHEJ [17,28,29], although the relative importance of each non-B DNA structure is largely unknown.

Subsequent triplication and haplotype modification can develop from the Japanese founder duplication through unequal interchromatid and interchromosomal recombinations [17,20]. Indeed, a tandem triplication with the [A-14] + [A-14] + [A-14] haplotype can be generated by unequal exchange between sister chromatids with the [A-14] + [A-14] haplotype, and various haplotype patterns are yielded by unequal interchromosomal exchanges involving the duplicated or triplicated segments. Furthermore, the haplotype variation would be facilitated by unequal exchanges between sister chromatids harboring duplications/triplications with various haplotype patterns and by the further unequal interchromosomal exchanges.

Underlying factors for the phenotypic variability

The duplications/triplications were accompanied by limb malformations with variable expressivity and incomplete penetrance. Although this may suggest the presence of a possible modifier(s) for the development of limb malformations, such a modifier(s) was not detected. In particular, while patient-to-carrier transmission of duplications/triplications was not identified in this study, even patient-to-carrier-to-patient transmission has been reported in three pedigrees [5,6,10]. Such transmission pattern with incomplete penetrance characterized by skipping of a generation is apparently inexplicable by assuming a modifier (s) interacting with *BHLHA9* or independent of *BHLHA9* on the duplication/triplication positive chromosome 17, on the normal chromosome 17, or on other chromosomes (Figure 3, Models A, B, and C, see also the legends in Figure 3).

In this regard, it is noteworthy that the development of limb malformations is obviously dependent on the size of genomic segment subjected to copy number gains. Actually, limb malformation has occurred in only one of 21 large duplications encompassing *BHLHA9* (average 1.55 Mb, mean 1.12 Mb) and in 29 of 80 small duplications encompassing *BHLHA9* (average 244 kb, mean 263 kb) ($P = 5.9 \times 10^{-3}$) [8]. Consistent with this, the patients with large and

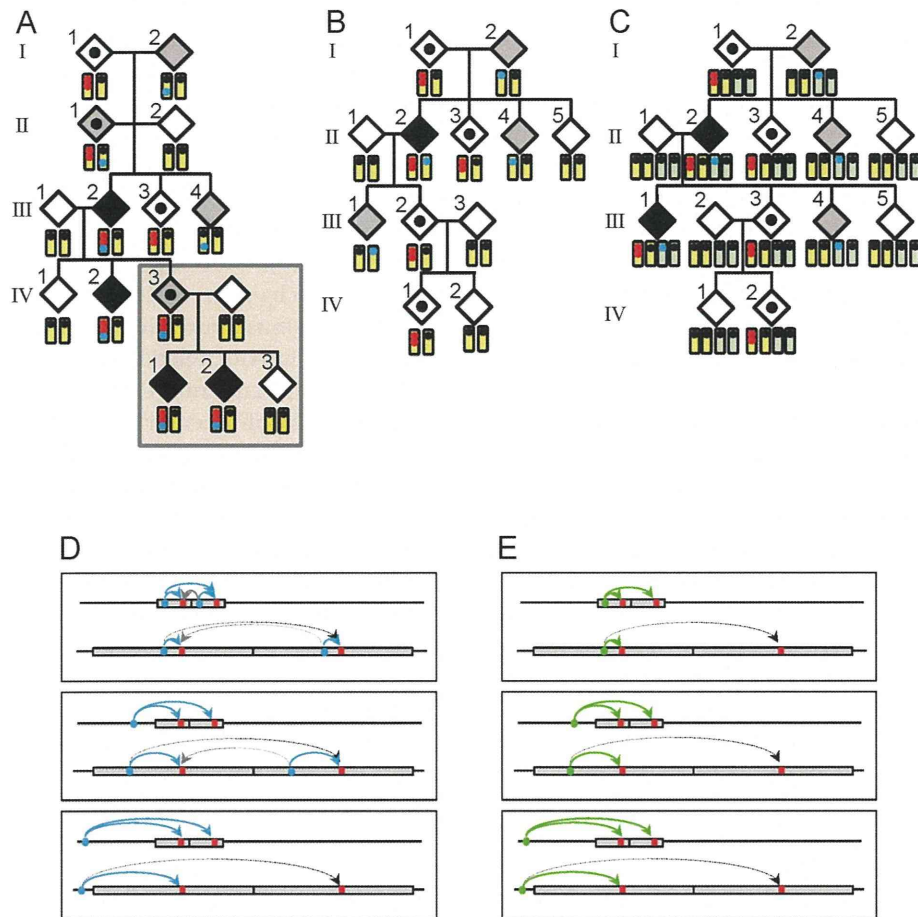


Figure 3 Models for a modifier(s) and effects of the duplication size. In models A–C, the yellow bars show chromosome 17, and the light green bars indicate other chromosomes. The two red dots represent the duplication at 17p13.3, and the blue dots indicate a putative modifier(s). Black painted diamonds represent limb malformation positive patients, dot-associated and gray painted diamonds indicate clinically normal carriers with the duplications and the modifier(s) respectively, and white painted diamonds denote clinically normal subjects without both the duplications and the modifier(s). **A.** This model assumes that co-existence of the duplication and a *cis*-acting modifier(s) causes limb malformation. If co-existence of the duplication and the *cis*-acting modifier(s) is associated with incomplete penetrance, this can explain all the transmission patterns observed to date, including the patient-to-carrier transmission and the presence of ≥ 2 affected children. **B.** This model postulates that the presence of a *cis*-acting modifier(s) on the normal chromosome 17 leads to limb malformation by enhancing the expression of the single *BHLHA9*, together with duplicated *BHLHA9* on the homologous chromosome. **C.** This model postulates that co-existence of the duplication at 17p13.3 and a modifier(s) on other chromosome causes limb malformation. In models D–E, the red bars represent *BHLHA9*, the blue circles indicate a physiological *cis*-regulatory element for *BHLHA9*, and the green circles indicate a non-physiological modifier(s) for *BHLHA9*. **D.** The physiological *cis*-regulatory element may be duplicated or non-duplicated, depending on its position relative to the size of the duplications. *BHLHA9* expression can be higher in small duplications than large duplications. **E.** The non-physiological modifier(s) can be transferred to various positions of the duplication positive chromosome 17, depending on the recombination places (see Model A). *BHLHA9* expression can be higher in small duplications than large duplications irrespective of the position of the modifier(s).

small duplications were ascertained primarily due to developmental retardation and limb malformation, respectively [8]. It is likely that a physiological *cis*-regulatory element for *BHLHA9* (e.g., an enhancer) can frequently but not invariably work on both of the duplicated *BHLHA9* when the duplication size is small but is usually incapable of working on duplicated *BHLHA9* when the duplication size is large, probably because of the difference in the chromatin structure (see Model D in Figure 3). Similar findings have also been reported in other genes. For example, small

(~150 kb) and relatively small (600–800 kb) duplications involving a putative testis-specific enhancer(s) for *SOX9* have caused 46,XX testicular and ovotesticular disorders of sex development respectively, whereas large duplications (~2 Mb) involving the enhancer(s) have permitted normal ovarian development in 46,XX individuals [30].

Thus, a plausible explanation may be that a range of limb malformations emerge when the effects of *BHLHA9* overdosage exceed the threshold for the development of SHFM, SHFLD, or GWC, depending on the conditions of

other genetic and environmental factors including the size of duplications/triplications as an important but not definitive factor. One may argue that this notion is inconsistent with the apparent anticipation phenomenon that is suggested by the rare patient-to-carrier transmission and the frequent carrier-to-patient transmission of the duplications/triplications, because no specific factor(s) exaggerating the development of limb malformations is postulated in the next generation. However, the skewed transmission pattern would primarily be ascribed to ascertainment bias rather than anticipation [31]. Indeed, while clinically normal parents of disease positive children would frequently be examined for the underlying genetic factor(s) of the children, clinically normal children born to disease positive parents would not usually be studied for such factor(s), as exemplified in this study. Similarly, the frequent patient-to-patient transmission of the duplications/triplications would also be ascribed to ascertainment bias, because molecular studies would preferentially be performed in such families. Nevertheless, the apparently autosomal dominant inheritance pattern of limb malformations in several families may still suggest the relevance of a non-physiological *cis*-acting modifier(s) (see Models A and E in Figure 3). It is possible that such a modifier(s), once transferred onto the duplication/triplication positive chromosome 17, is usually co-transmitted with the duplications/triplications, leading to a specific condition in which the effects of *BHLHA9* overdosage frequently but not invariably exceed the threshold for the development of limb malformations in offsprings with the duplications/triplications.

Remarks

Several matters should be pointed out in the present study. First, in contrast to diverse duplication sizes in non-Japanese populations [5-9], the size of the genomic segment subjected to duplications/triplications was identical in this study. Since families 1–27 were derived from various places of Japan, there is no selection bias in terms of a geographic distribution. Rather, since the small duplications/triplications identified in this study were not associated with developmental retardation, it is likely that they spread throughout Japan primarily via carriers with normal fitness and were found via patients with limb malformations. Obviously, this notion does not exclude the possible presence of other types of duplications/triplications at 17p13.3 in Japan. Second, except for the duplications/triplications at 17p13.3, we could reveal a homozygous *WNT10B* mutation (SHFM6) only in a single SHFM family and chromosome 10q24 duplications (SHFM3) only in three SHFM families. Thus, underlying factors are still unknown in the remaining 20 families, although tiny deletions and/or duplications affecting the known SHFM loci might have

been overlooked because of the low resolution of the array. In addition, although all the probands had a normal karyotype, there might be cryptic translocations and/or inversions involving the known SHFM loci. Third, no deletion of *BHLHA9* was identified in the 51 probands and in the 200 control subjects. This argues against the relevance of *BHLHA9* haploinsufficiency to limb malformations, and coincides with the Japanese founder duplication being produced by a replication-mediated mechanism rather than an interchromatid/interchromosomal (but not an intrachromatid) NAHR that can lead to both deletions and duplications as a mirror image [17]. Furthermore, it remains to be determined (i) whether gain-of-function mutations (and possibly loss-of-function mutations as well) of *BHLHA9* are identified in patients with limb malformations, (ii) whether duplications/triplications involving *BHLHA9* underlie limb malformations other than SHFM, SHFLD, and GWC, and (iii) whether *BHLHA9*-containing duplications/triplications are also the most frequent underlying factors for limb malformations in non-Japanese populations.

Conclusions

The results imply that (i) duplications/triplications involving *BHLHA9* at chromosome 17p13.3 constitute a strong susceptibility factor for the development of a range of limb malformations including SHFM, SHFLD, and GWC; (ii) the Japanese founder duplication was generated by a replication-based mechanism and spread with subsequent triplication and haplotype modification through recombination-based mechanisms; and (iii) clinical variability appears to be due to multiple factors including the size of duplications/triplications. Thus, the present study provides useful information on the development of limb malformations.

Additional files

Additional file 1: Table S1. Primers utilized in this study.

Additional file 2: Figure S1. Real-time PCR analysis.

Additional file 3: Figure S2. *D17S1174* analysis in 200 Japanese control subjects, showing discontinuous distribution of the CA repeat numbers, as observed in the Japanese families with limb malformations.

Additional file 4: Table S2. *In silico* analysis for specific structures around the breakpoint-flanking regions and control regions.

Additional file 5: Table S3. Phenotypes in patients/subjects with increased copy number of *BHLHA9*.

Additional file 6: Figure S3. Genomic region encompassing *BHLHA9* examined in this study.

Additional file 7: Table S4. Polymorphism analysis of rs3951819 (A/G SNP) in *BHLHA9*.

Additional file 8: Table S5. Polymorphism analysis of rs34201045 (4 bp insertion) in *TP63*.

Additional file 9: Figure S4. Genomic basis of the Japanese founder copy number gain.

Abbreviations

AER: Apical ectodermal ridge; CEP17: Centromere of chromosome 17; CGH: Comparative genomic hybridization; Dup: Duplication; FoSTeS: Fork stalling and template switching; GWC: Gollop-Wolfgang complex; L: Lower; LBD: Long bone defect; MMBIR: Microhomology-mediated break-induced replication; NAHR: Non-allelic homologous recombination; N.E.: Not examined; NHEJ: Non-homologous end-joining; qPCR: Quantitative real-time PCR; SF: Split foot 17j; SH: Split hand; SHFLD: SHFM with long bone deficiency; SHFM: Split-hand/foot malformation; Trip: Triplication; U: Upper.

Competing interests

The authors have nothing to declare.

Authors' contributions

Molecular analysis using human samples was performed by EN, HK, FK, RY, SN, SW, KY, TT, SS, MF, and TT, ST, and SY; clinical assessment and blood sampling by RK, HT, SM, TK, TH, MK, AS, KS, HO, NH, HN, EH, TN, HY, GN, and TO; design of this study and interpretations of the data by HA, SI, and TO; and paper writing by TO. All authors read and approved the final manuscript.

Acknowledgements

This work was supported in part by Grants-in-Aid for Scientific Research on Innovative Areas [22132004-A01] from the Ministry of Education, Culture, Sports, Science and Technology, by Grant for Research on Intractable Diseases from the Ministry of Health, Labor and Welfare [H24-048], and by Grants from National Center for Child Health and Development [23A-1, 24-7]. The funders had no role in study design, data collection and analysis, decision to publish, or preparation of the manuscript.

Author details

¹Department of Pediatrics, Hamamatsu University School of Medicine, Hamamatsu 431-3192, Japan. ²Laboratory of Bone and Joint Diseases, Center for Integrative Medical Sciences, RIKEN, Tokyo, Japan. ³Department of Orthopedic Surgery, Tokyo, Japan. ⁴Division of Medical Genetics, National Center for Child Health and Development, Tokyo, Japan. ⁵Section of Clinical Genetics, Department of Pediatrics, Tenshi Hospital, Sapporo, Japan. ⁶Department of Pediatrics, Central Hospital, Aichi Human Service Center, Kasugai, Japan. ⁷Department of Human Genetics, Nagasaki University Graduate School of Biomedical Sciences, Nagasaki, Japan. ⁸Department of Medical Genetics, Shinshu University School of Medicine, Matsumoto, Japan. ⁹Department of Pediatrics, Keio University School of Medicine, Tokyo, Japan. ¹⁰Department of Orthopedics, National Rehabilitation Center for Disabled Children, Tokyo, Japan. ¹¹Division of Medical Genetics, Saitama Children's Medical Center, Saitama, Japan. ¹²Department of Rehabilitation Medicine, University of Tokyo, Tokyo, Japan. ¹³Department of Genetic Counseling, Graduate School of Humanities and Sciences, Ochanomizu University, Tokyo, Japan. ¹⁴Department of Orthopedic Surgery, Japanese Red Cross Nagoya Daiichi Hospital, Nagoya, Japan. ¹⁵Department of Pediatrics, Dokkyo Medical University Koshigaya Hospital, Koshigaya, Japan. ¹⁶Division of Medical Genetics, Tokyo, Japan. ¹⁷Department of Pediatric Imaging, Tokyo Metropolitan Children's Medical Center, Tokyo, Japan. ¹⁸Division of Neurology/Molecular Brain Science, Kobe University Graduate School of Medicine, Kobe, Japan. ¹⁹Department of Systems Biomedicine, National Research Institute for Child Health and Development, Tokyo, Japan. ²⁰Department of Systems Biomedicine, Graduate School of Medical and Dental Sciences, Tokyo Medical and Dental University, Tokyo, Japan. ²¹Department of Molecular Endocrinology, National Research Institute for Child Health and Development, Tokyo, Japan. ²²Present address: Laboratory of Metabolism Center for Cancer Research, National Cancer Institute, Bethesda, MD, USA.

Received: 15 April 2014 Accepted: 22 July 2014

Published online: 21 October 2014

References

1. Duijff PH, van Bokhoven H, Brunner HG: Pathogenesis of split-hand/split-foot malformation. *Hum Mol Genet* 2003, **12**:R51-60.
2. Gurrieri F, Everman DB: Clinical, genetic, and molecular aspects of split-hand/foot malformation: an update. *Am J Med Genet A* 2013, **161A**:2660-2672.

3. Lango Allen H, Caswell R, Xie W, Xu X, Wragg C, Turnpenny PD, Turner CL, Weedon MN, Ellard S: Next generation sequencing of chromosomal rearrangements in patients with split-hand/split-foot malformation provides evidence for DYNC11/1 exonic enhancers of DLX5/6 expression in humans. *J Med Genet* 2014, **51**:264-267.
4. Lezirovitz K, Maestrelli SR, Cotrim NH, Otto PA, Pearson PL, Mingroni-Netto RC: A novel locus for split-hand/foot malformation associated with tibial hemimelia (SHFLD syndrome) maps to chromosome region 17p13.1-17p13.3. *Hum Genet* 2008, **123**:625-631.
5. Armour CM, Bulman DE, Jarinova O, Rogers RC, Clarkson KB, DuPont BR, Dwivedi A, Bartel FO, McDonnell L, Schwartz CE, Boycott KM, Everman DB, Graham GE: 17p13.3 microduplications are associated with split-hand/foot malformation and long-bone deficiency (SHFLD). *Eur J Hum Genet* 2011, **19**:1144-1151.
6. Klopocki E, Lohan S, Doelken SC, Stricker S, Ockeloen CW, Soares Thiele de Aguiar R, Lezirovitz K, Mingroni Netto RC, Jamsheer A, Shah H, Kurth I, Habenicht R, Warman M, Devriendt K, Kordass U, Hempel M, Rajab A, Mäkitie O, Naveed M, Radhakrishna U, Antonarakis SE, Horn D, Mundlos S: Duplications of BHLHA9 are associated with ectrodactyly and tibia hemimelia inherited in non-Mendelian fashion. *J Med Genet* 2012, **49**:119-125.
7. Petit F, Andrieux J, Demeer B, Collet LM, Copin H, Boudry-Labis E, Escande F, Manouvrier-Hanu S, Mathieu-Dramard M: Split-hand/foot malformation with long-bone deficiency and BHLHA9 duplication: two cases and expansion of the phenotype to radial agenesis. *Eur J Med Genet* 2013, **56**:88-92.
8. Curry CJ, Rosenfeld JA, Grant E, Gripp KW, Anderson C, Aylsworth AS, Saad TB, Chizhikov W, Dybose G, Fagerberg C, Falco M, Fels C, Fichera M, Graakjaer J, Greco D, Hair J, Hopkins E, Huggins M, Ladda R, Li C, Moeschler J, Nowaczyk MJ, Ozmore JR, Reitano S, Romano C, Roos L, Schnur RE, Sell S, Suwannarat P, Svaneby D, et al: The duplication 17p13.3 phenotype: analysis of 21 families delineates developmental, behavioral and brain abnormalities, and rare variant phenotypes. *Am J Med Genet A* 2013, **161A**:1833-1852.
9. Luk HM, Wong VC, Lo IF, Chan KY, Lau ET, Kan AS, Tang MH, Tang WF, She WM, Chu YW, Sin WK, Chung BH: A prenatal case of split-hand malformation associated with 17p13.3 triplication - a dilemma in genetic counseling. *Eur J Med Genet* 2014, **57**:81-84.
10. Petit F, Jourdain AS, Andrieux J, Baujat G, Baumann C, Beneteau C, David A, Faivre L, Gaillard D, Gilbert-Dussardier B, Jouk PS, Le Caignec C, Loget P, Pasquier L, Porchet N, Holder-Espinasse M, Manouvrier-Hanu S, Escande F: Split hand/foot malformation with long-bone deficiency and BHLHA9 duplication: report of 13 new families. *Clin Genet* 2014, **85**:464-469.
11. Kano H, Kurosawa K, Horii E, Ikegawa S, Yoshikawa H, Kurahashi H, Toda T: Genomic rearrangement at 10q24 in non-syndromic split-hand/split-foot malformation. *Hum Genet* 2005, **118**:477-483.
12. Matsuyama J, Mabuchi A, Zhang J, Iida A, Ikeda T, Kimizuka M, Ikegawa S: A pair of sibs with tibial hemimelia born to phenotypically normal parents. *J Hum Genet* 2003, **48**:173-176.
13. Kagami M, Sekita Y, Nishimura G, Irie M, Kato F, Okada M, Yamamori S, Kishimoto H, Nakayama M, Tanaka Y, Matsuoka K, Takahashi T, Noguchi M, Tanaka Y, Masumoto K, Utsunomiya T, Kouzan H, Komatsu Y, Ohashi H, Kurosawa K, Kosaki K, Ferguson-Smith AC, Ishino F, Ogata T: Deletions and epimutations affecting the human 14q32.2 imprinted region in individuals with paternal and maternal upd(14)-like phenotypes. *Nat Genet* 2008, **40**:237-242.
14. Iida A, Okamoto N, Miyake N, Nishimura G, Minami S, Sugimoto T, Nakashima M, Tsurusaki Y, Saitsu H, Shiina M, Ogata K, Watanabe S, Ohashi H, Matsumoto N, Ikegawa S: Exome sequencing identifies a novel INPPL1 mutation in opsismodysplasia. *J Hum Genet* 2013, **58**:391-394.
15. Cer RZ, Donohue DE, Mudunuri US, Temiz NA, Loss MA, Starner NJ, Halusa GN, Volfovsky N, Yi M, Luke BT, Bacolla A, Collins JR, Stephens RM: Non-B DNA motifs: a database of predicted non-B DNA-forming motifs and its associated tools. *Nucl Acids Res* 2013, **41**:D94-D100.
16. Kornreich R, Bishop DF, Desnick RJ: α -Galactosidase A gene rearrangements causing Fabry disease: identification of short direct repeats at breakpoints in an Alu-rich gene. *J Biol Chem* 1990, **265**:9319-9326.
17. Gu W, Zhang F, Lupski JR: (2008) Mechanisms for human genomic rearrangements. *Pathogenetics* 2008, **1**:4.
18. Vissers LE, Bhatt SS, Janssen IM, Xia Z, Lalani SR, Pfundt R, Derwinski K, de Vries BB, Gilissen C, Hoischen A, Nesteruk M, Wisniewicka-Kowalik B, Smyk

- M, Brunner HG, Cheung SW, van Kessel AG, Veltman JA, Stankiewicz P: Rare pathogenic microdeletions and tandem duplications are microhomology-mediated and stimulated by local genomic architecture. *Hum Mol Genet* 2009, **18**:3579–3593.
19. Hastings PJ, Ira G, Lupski JR: A microhomology-mediated break-induced replication model for the origin of human copy number variation. *PLoS Genet* 2009, **5**:e1000327.
 20. Colnaghi R, Carpenter G, Volker M, O'Driscoll M: The consequences of structural genomic alterations in humans: genomic disorders, genomic instability and cancer. *Semin Cell Dev Biol* 2011, **22**:875–885.
 21. Ugur SA, Tolun A: Homozygous WNT10b mutation and complex inheritance in Split-Hand/Foot Malformation. *Hum Mol Genet* 2008, **17**:2644–2653.
 22. Oort PJ, Warden CH, Baumann TK, Knotts TA, Adams SH: Characterization of *Tusc5*, an adipocyte gene co-expressed in peripheral neurons. *Mol Cell Endocrinol* 2007, **276**:24–35.
 23. Manning JT, Scutt D, Wilson J, Lewis-Jones DJ: The ratio of 2nd to 4th digit length: a predictor of sperm numbers and concentrations of testosterone, luteinizing hormone and oestrogen. *Hum Reprod* 1998, **13**:3000–3004.
 24. Manning JT, Trivers RL, Singh D, Thornhill R: The mystery of female beauty. *Nature* 1999, **399**:214–215.
 25. Williams TJ, Pepitone ME, Christensen SE, Cooke BM, Huberman AD, Breedlove NJ, Breedlove TJ, Jordan CL, Breedlove SM: Finger-length ratios and sexual orientation. *Nature* 2000, **404**:455–456.
 26. Heald AH, Ivison F, Anderson SG, Cruickshank K, Laing I, Gibson JM: Significant ethnic variation in total and free testosterone concentration. *Clin Endocrinol* 2003, **58**:262–266.
 27. Manning JT, Stewart A, Bundred PE, Trivers RL: Sex and ethnic differences in 2nd to 4th digit ratio of children. *Early Hum Dev* 2004, **80**:161–168.
 28. Wang G, Vasquez KM: Non-B DNA structure-induced genetic instability. *Mutat Res* 2006, **598**:103–119.
 29. Zhao J, Bacolla A, Wang G, Vasquez KM: Non-B DNA structure-induced genetic instability and evolution. *Cell Mol Life Sci* 2010, **67**:43–62.
 30. Benko S, Gordon CT, Mallet D, Sreenivasan R, Thauvin-Robinet C, Brendehaug A, Thomas S, Bruland O, David M, Nicolino M, Labalme A, Sanlaville D, Callier P, Malan V, Huet F, Molven A, Djoud F, Munnich A, Faivre L, Amiel J, Harley V, Houge G, Morel Y, Lyonnet S: Disruption of a long distance regulatory region upstream of *SOX9* in isolated disorders of sex development. *J Med Genet* 2011, **48**:825–830.
 31. Fraser FC: Trinucleotide repeats not the only cause of anticipation. *Lancet* 1997, **350**:459–460.

doi:10.1186/s13023-014-0125-5

Cite this article as: Nagata et al.: Japanese founder duplications/triplications involving *BHLHA9* are associated with split-hand/foot malformation with or without long bone deficiency and Gollop-Wolfgang complex. *Orphanet Journal of Rare Diseases* 2014 **9**:125.

Submit your next manuscript to BioMed Central and take full advantage of:

- Convenient online submission
- Thorough peer review
- No space constraints or color figure charges
- Immediate publication on acceptance
- Inclusion in PubMed, CAS, Scopus and Google Scholar
- Research which is freely available for redistribution

Submit your manuscript at
www.biomedcentral.com/submit

